Supplementary Data

Copper(II) Bis(oxamato) End-grafted (Poly)Amidoamine Dendrimers

Karoline Rühlig,[a] Robert Mothes,[a] Azar Aliabadi,[b] Vladislav Kataev,[b] Bernd Büchner,[b] Roy Buschbeck,[a] Tobias Rüffer,[a*] and Heinrich Lang[a]

[a] *Technische Universität Chemnitz, Faculty of Natural Sciences, Institute of Chemistry, Inorganic Chemistry, 09107 Chemnitz, Germany*

[b] *Leibniz Institute for Solid State and Materials Research IFW Dresden, Helmholtzstraße 20, 01069 Dresden.*

Contents

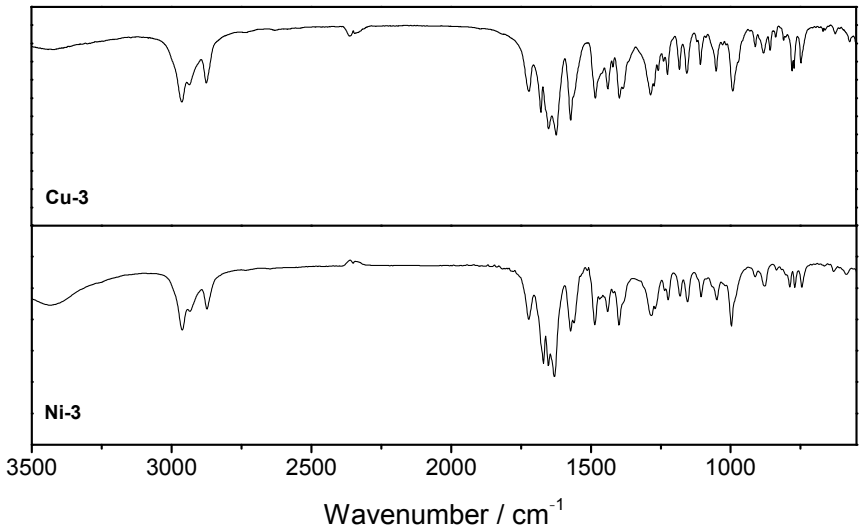

Figure S 1. IR spectra of **Cu-3** and **Ni-3** (KBr).

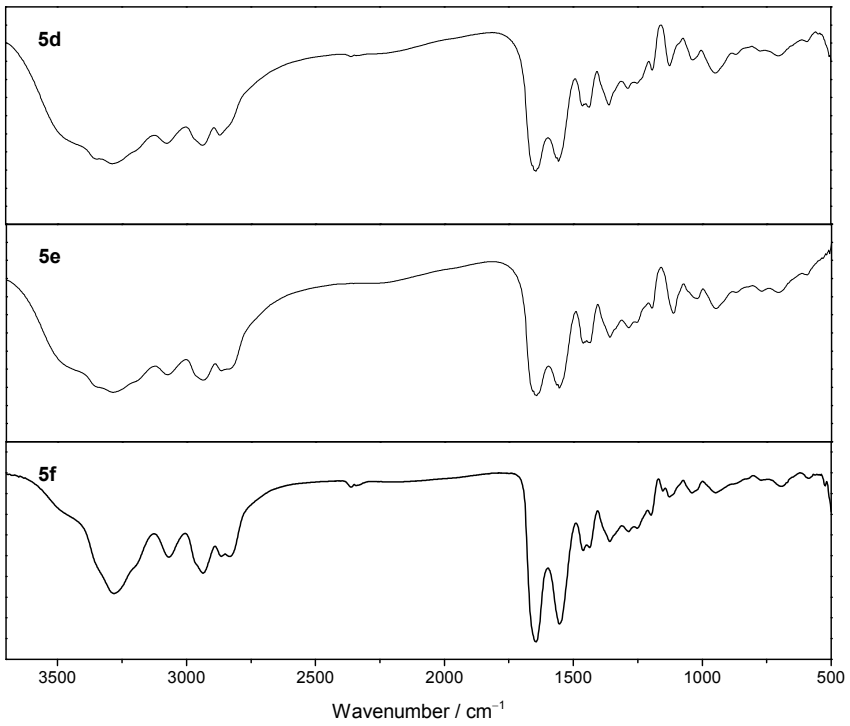

Figure S 2. IR spectra of **5d-f** (NaCl).

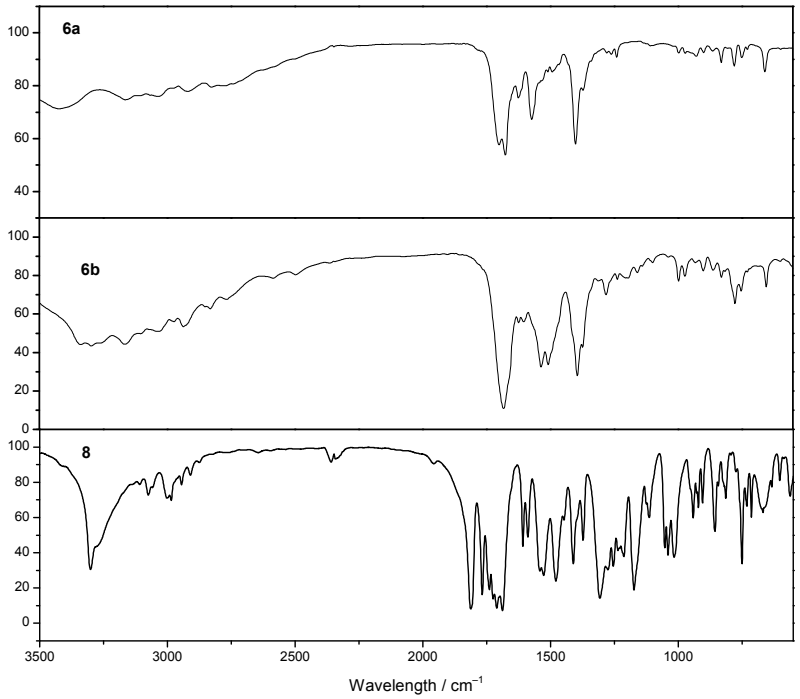

Figure S 3. IR spectra of **6a**,**b** and **8** (KBr).

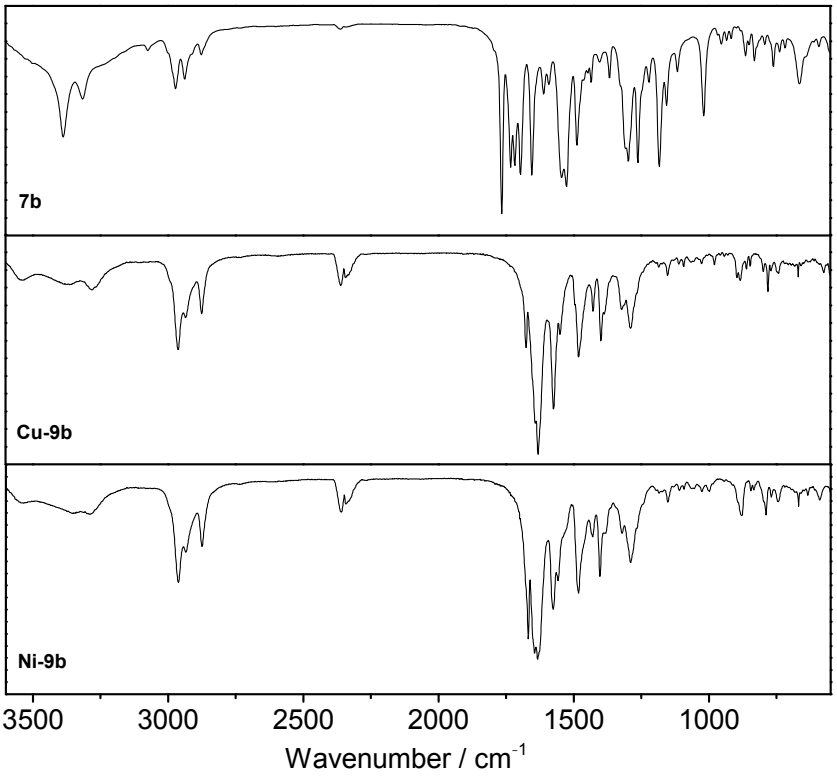

Figure S 4. IR spectra of **7b**, **Cu-9b** and **Ni-9b** (KBr).

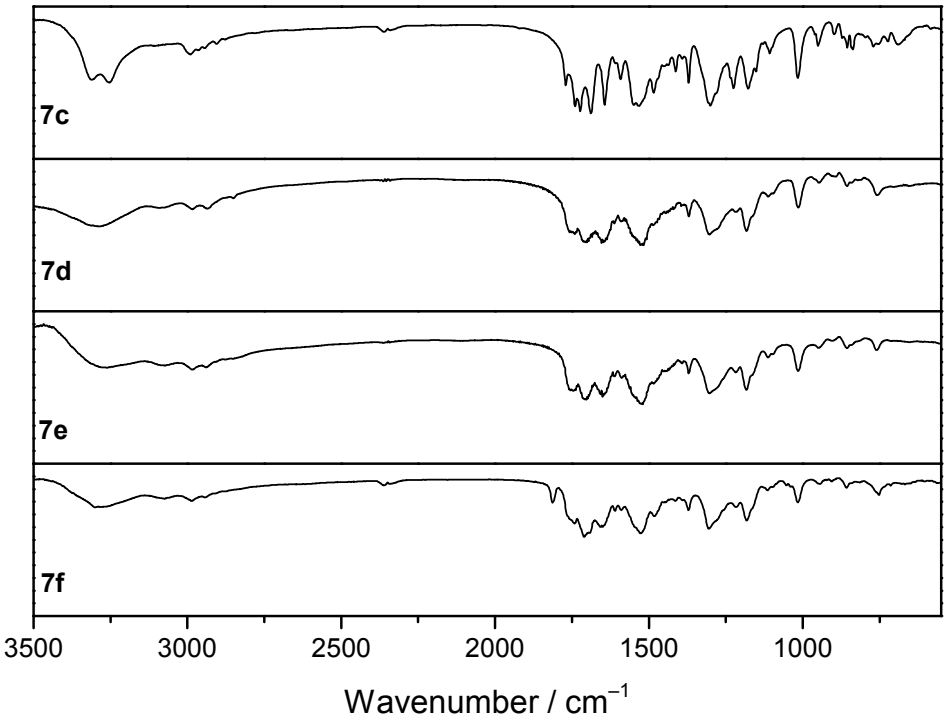

Figure S 5. IR spectra of **7c–f (**KBr).

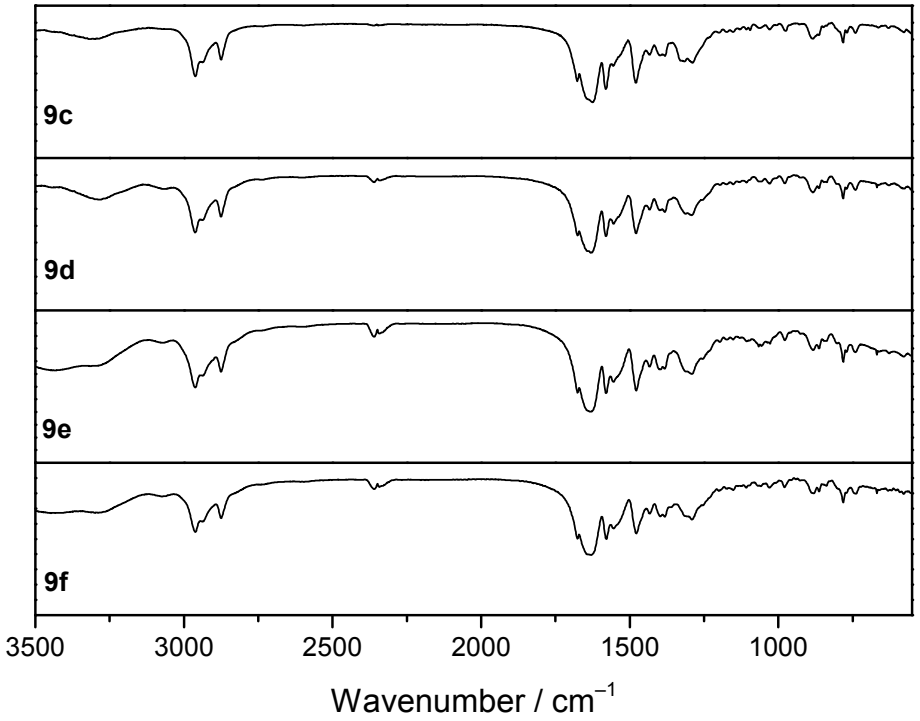

Figure S 6. IR spectra of **9c–9f** (KBr).

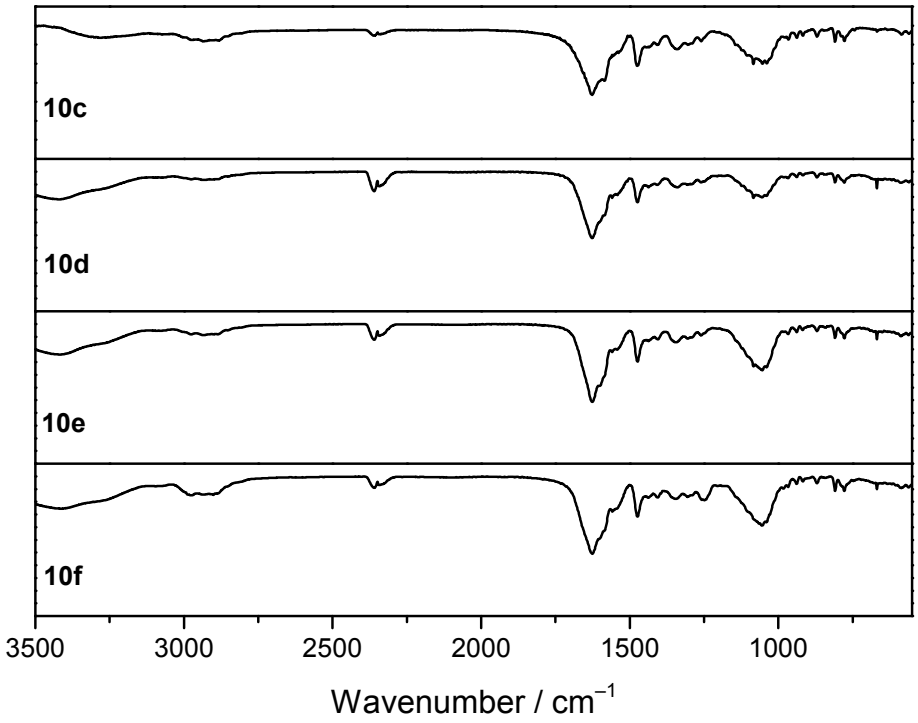

Figure S 7. IR spectra of **10c–f** (KBr).

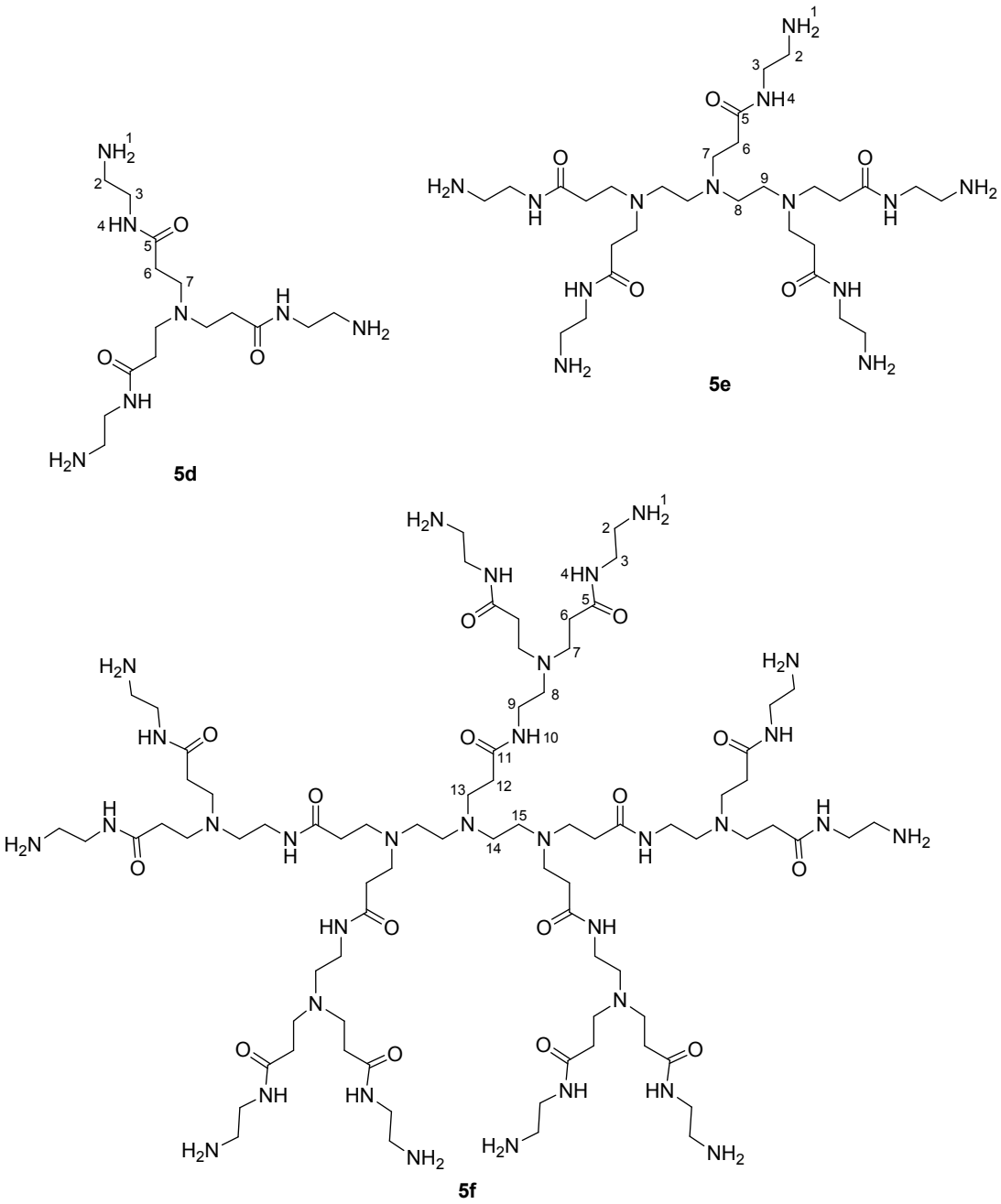

Figure S 8. Molecule numbering scheme for the ^{1}H and ^{13}C NMR spectroscopic characterisation of **5d**–**f**.

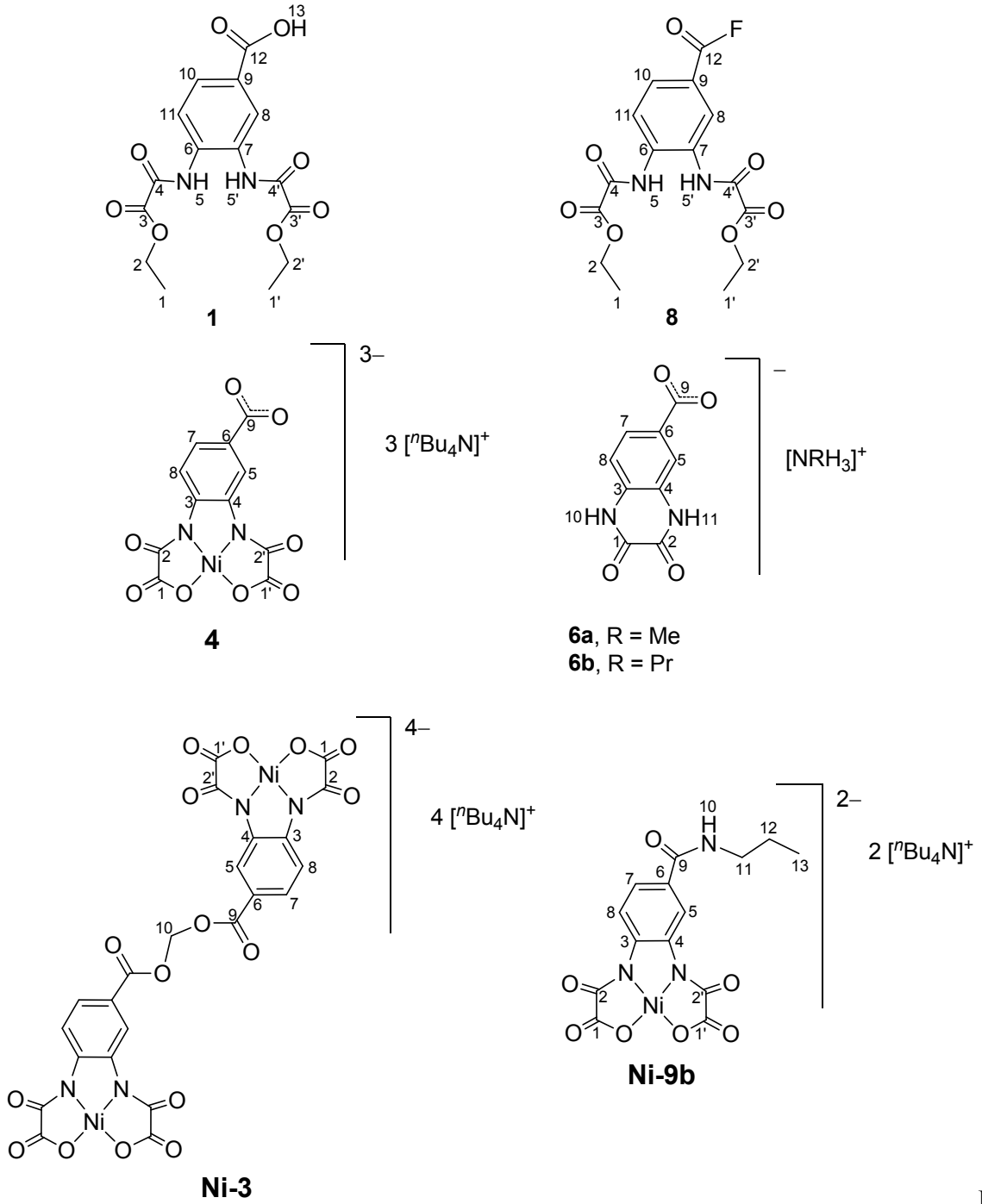

Figure S 9. Molecule numbering scheme for the ^{1}H and ^{13}C NMR spectroscopic characterisation of **1**, **8**, **4**, **6a**,**b**, **Ni-3** and **Ni-9b**.

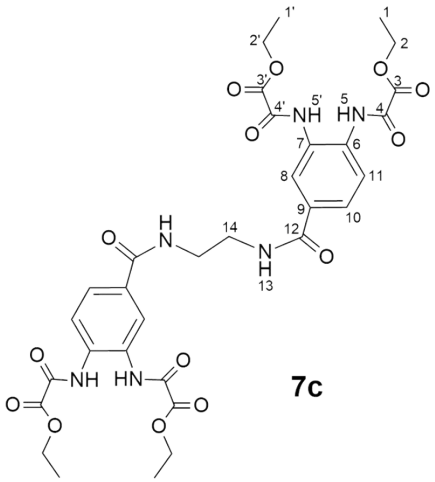

7c

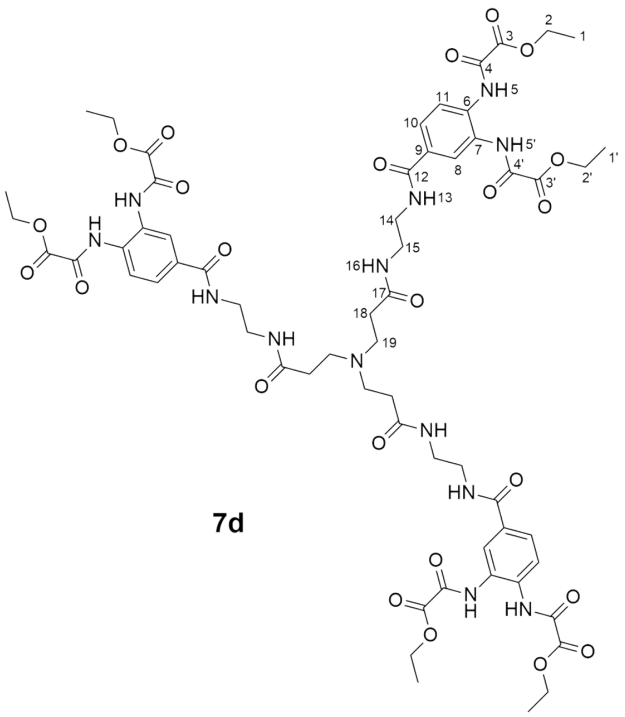

7d

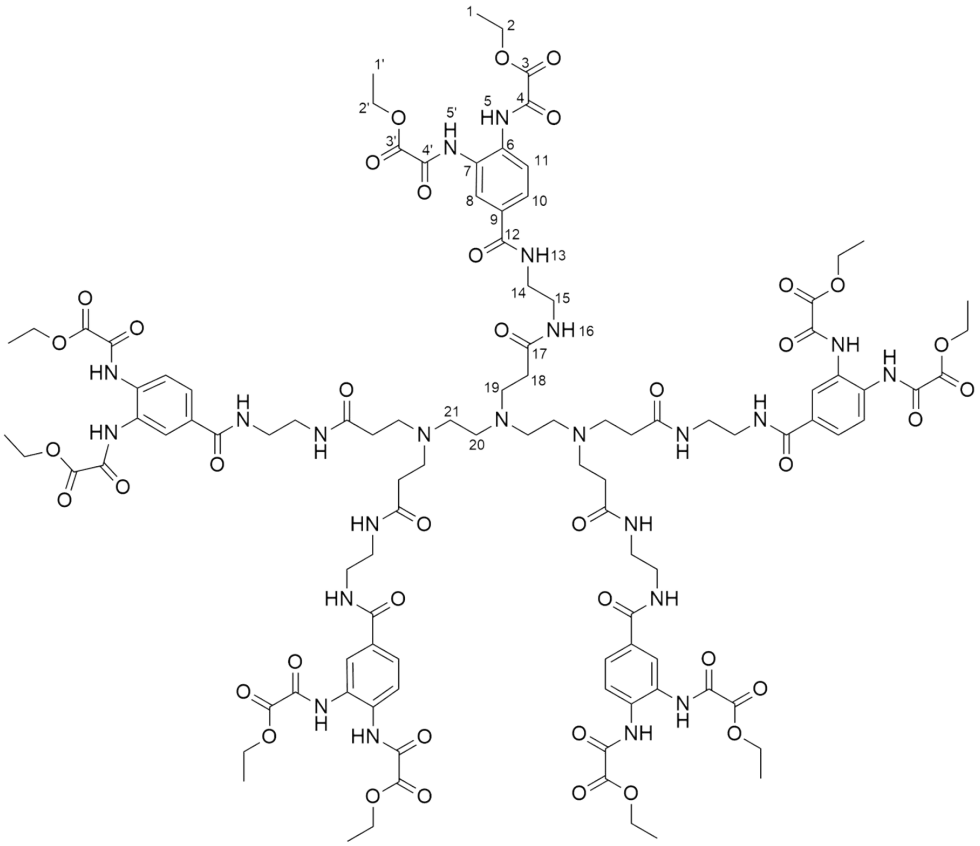

7e

Figure S 10. Molecule numbering scheme for the ^{1}H and ^{13}C NMR spectroscopic characterisation of **7d**–**f**.

*Characterisation of **1**,[1] **5d**[2,3] and **5e**[2,3]:*

1: ^{1}H NMR (dmso-d_6): δ 1.32/1.33 (t/t, $^{3}J_{H,H}$ = 7.1 Hz, 3H/3H, C$H^{1,1'}$), 4.32/4.33 (q/q, $^{3}J_{H,H}$ = 7.1 Hz, 2H/2H, C$H^{2,2'}$), 7.79 (d, $^{3}J_{H,H}$ = 9 Hz, 1H, CH^{11}), 7.86 (dd, $^{4}J_{H,H}$ = 1.9 Hz, $^{3}J_{H,H}$ = 9 Hz, 1H, CH^{10}), 8.13 (d, $^{4}J_{H,H}$ = 1.9 Hz, 1H, CH^{8}), 10.50/10.55 (s/s, 1H/1H, N$H^{5,5'}$), 13.10 (s, 1H, OH^{13}). ^{13}C{^{1}H} NMR (dmso-d_6): δ 13.8/13.8 (C$H^{1,1'}$), 62.6/62.6 (C$H^{2,2'}$), 125.0/127.0/127.3/128.3/ 129.2/133.9 (C^{Ph}), 155.5/155.8 (C$^{4,4'}$), 160.0/160.0 (C$^{3,3'}$), 166.3 (C^{12}).

den^{III}H$_3$ (**5d**): Anal. Calcd for $C_{15}H_{33}N_7O_3$ (359.5): C, 50.1; H, 9.3; N, 27.3 %. Found: C, 49.46; H, 9.63%; N, 27.34 %. ^{1}H NMR ($CDCl_3$): δ 1.49 (s, 6H, NH^{1}), 2.13/2.49 (t/t, $^{3}J_{H,H}$ = 6.1 Hz/$^{3}J_{H,H}$ = 6.2 Hz, 6H/6H,C$H^{6,7}$), 2.57/2.99–3.05 (t/m, $^{3}J_{H,H}$ = 6.0 Hz, 6H/6H, C$H^{2,3}$), 7.51 (s, 3H, NH^{4}). ^{13}C{^{1}H} NMR ($CDCl_3$): δ 34.4 (C$H^{7,6}$), 41.5 (C$H^{2,3}$), 42.3 (C$H^{2,3}$), 50.1 (C$H^{7,6}$), 173.0 (C^{5}).

den^{V}H$_5$ (**5e**): Anal. Calcd for $C_{29}H_{63}N_{13}O_5$ (673.9): C, 51.7; H, 9.4; N, 27.0 %. Found: C, 50.84; H, 9.69%; N, 26.16 %. ^{1}H NMR ($CDCl_3$) : δ 1.58 (s, 10H, NH^{1}), 2.28–2.33/2.62–2.67 (m/m, 10H/10H, C$H^{6,7}$), 2.39 (s, 8H, C$H^{8,9}$), 2.71–2.75/3.16–3.23 (m/m, 10H/10H, C$H^{2,3}$), 7.66/7.91 (t/t, $^{3}J_{H,H}$ = 5.7/5.6 Hz, 5H, NH^{4}). ^{13}C{^{1}H} NMR ($CDCl_3$): δ 34.3/34.3 (C$H^{8,9}$), 41.6 (C$H^{2,3}$), 42.4 (C$H^{2,3}$), 50.7/50.8 (C$H^{6,7}$), 52.1/52.3 (C$H^{8,9}$), 172.9/173.1 (C^{5}).

1 C. Paul-Roth, *Comptes Rendus Chim.*, 2005, **8**, 1232–1236.

2 D. A. Tomalia, *United States Patent 4507466, 1985.*, United States, 1985.

3 S. Dietrich, A. Nicolai and H. Lang, *J. Organomet. Chem.*, 2011, **696**, 739–747.

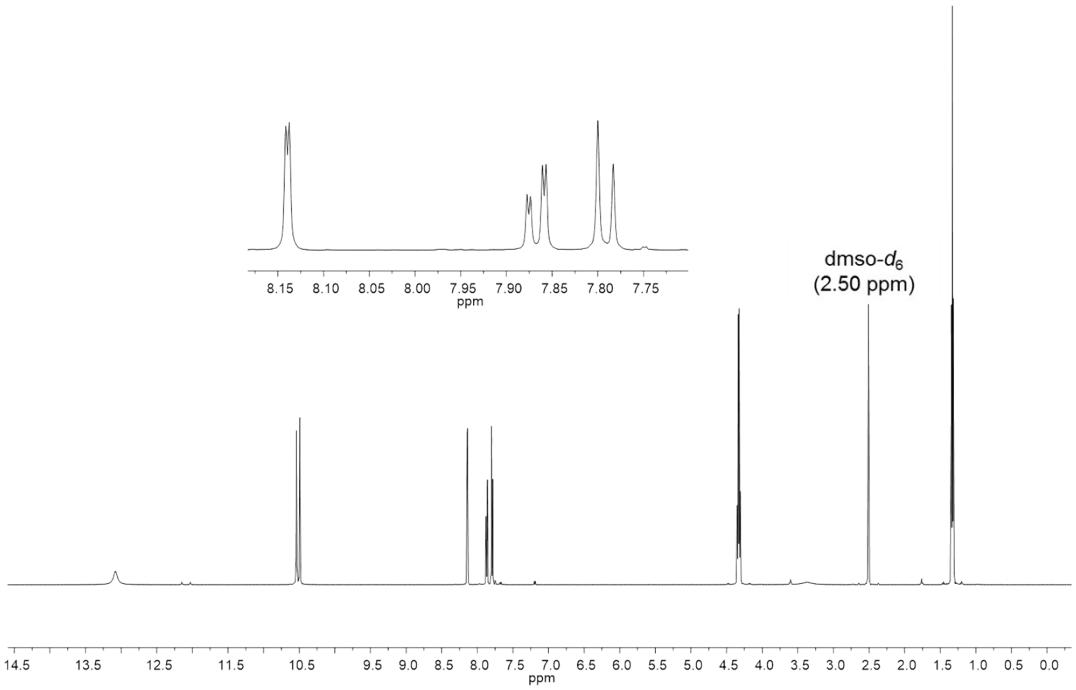

Figure S 11. ^{1}H NMR spectrum (dmso-d_6) of **1**.

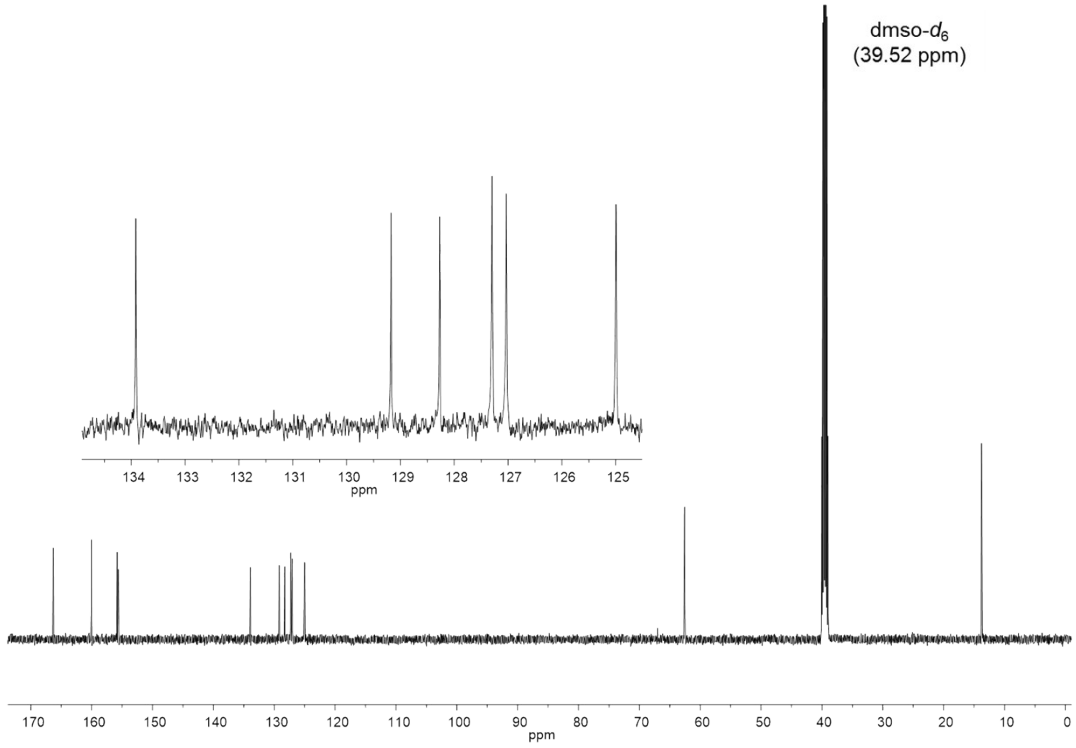

Figure S 12. ^{13}C{^{1}H} NMR spectrum (dmso-d_6) of **1**.

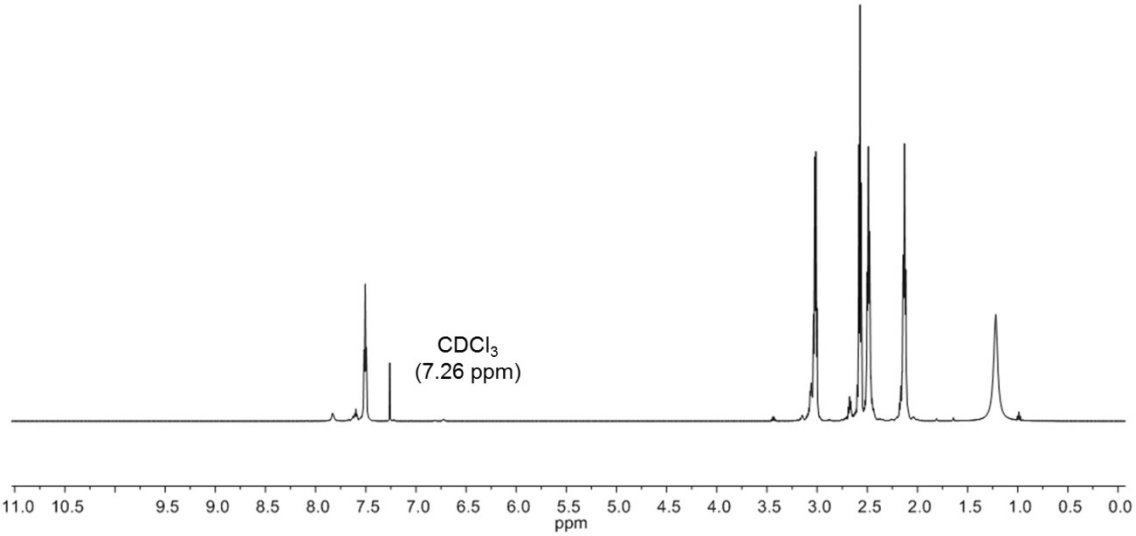

Figure S 13. ^{1}H NMR spectrum ($CDCl_3$) of **5d**.

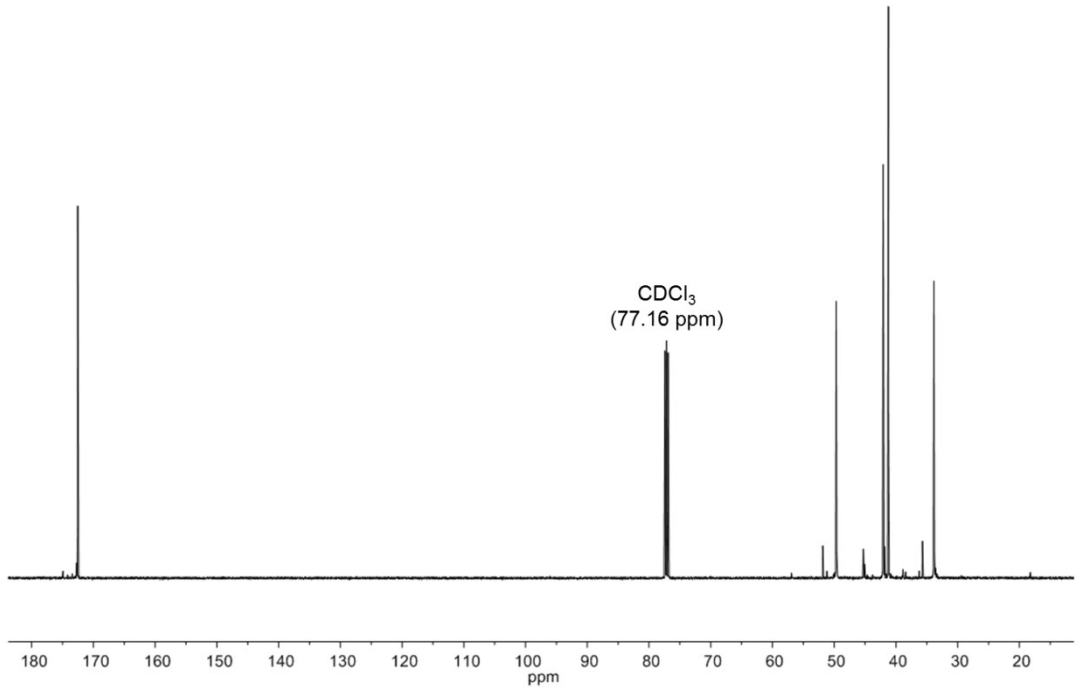

Figure S 14. $^{13}C\{^{1}H\}$ NMR spectrum ($CDCl_3$) of **5d**.

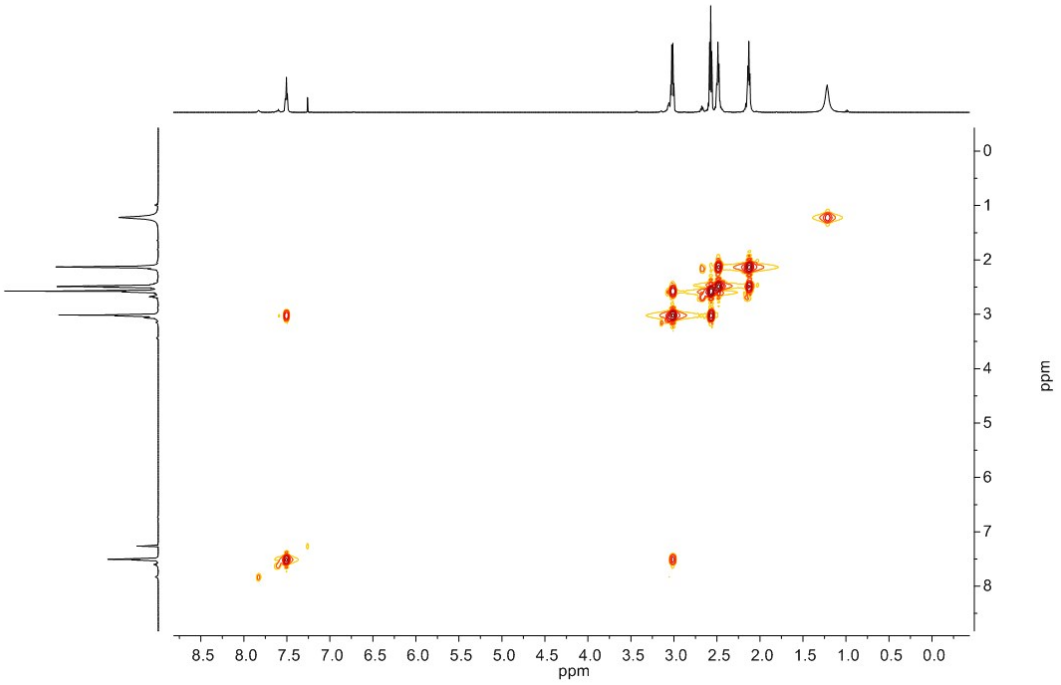

Figure S 15. $^{1}H,^{1}H$-COSYGPSW NMR spectrum ($CDCl_3$) of **5d**.

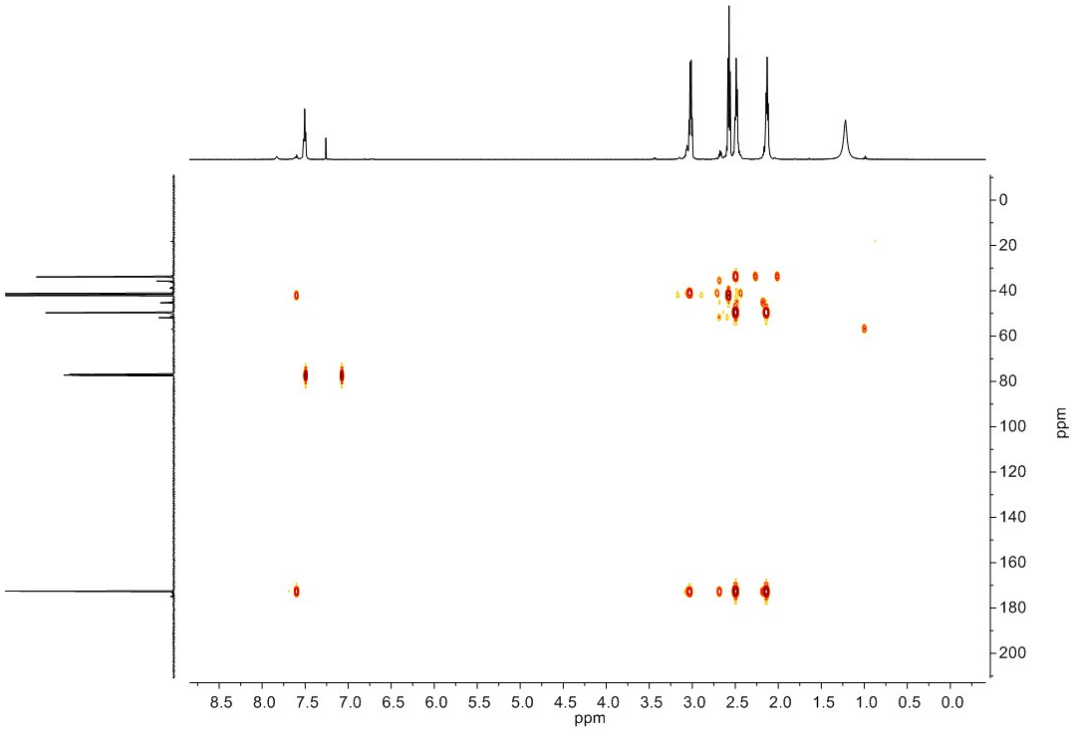

Figure S 16. $^{1}H,^{13}C$-HMBCGP NMR spectrum ($CDCl_3$) of **5d**.

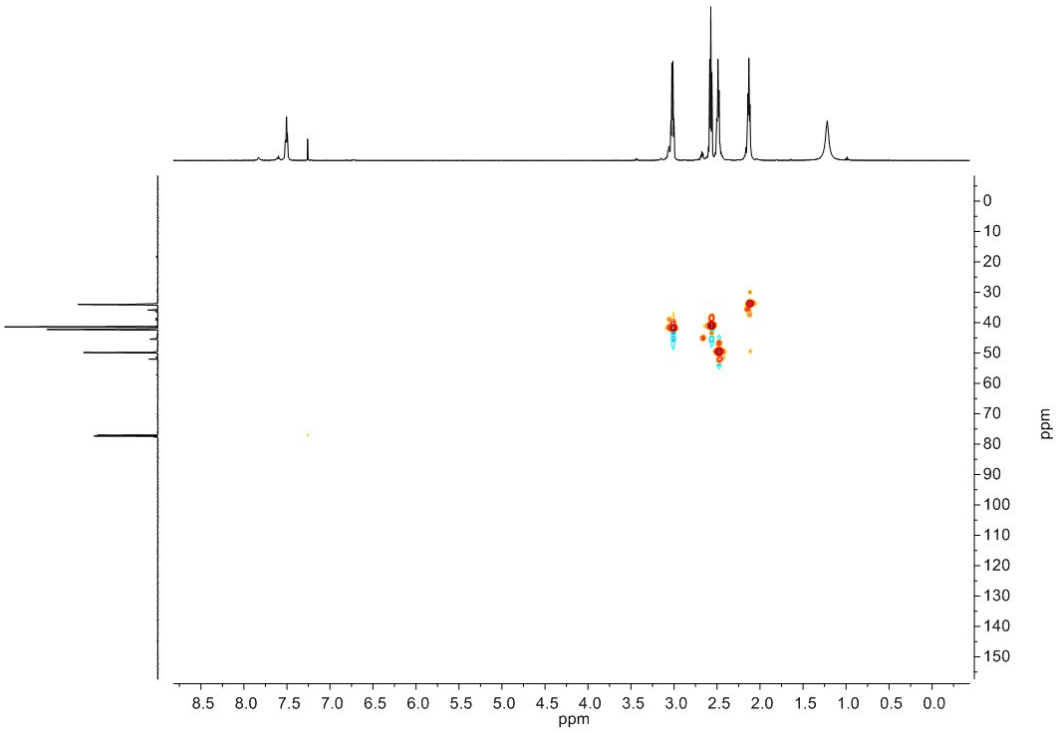

Figure S 17. $^{1}H,^{13}C$-HSQCETGP NMR spectrum ($CDCl_3$) of **5d**.

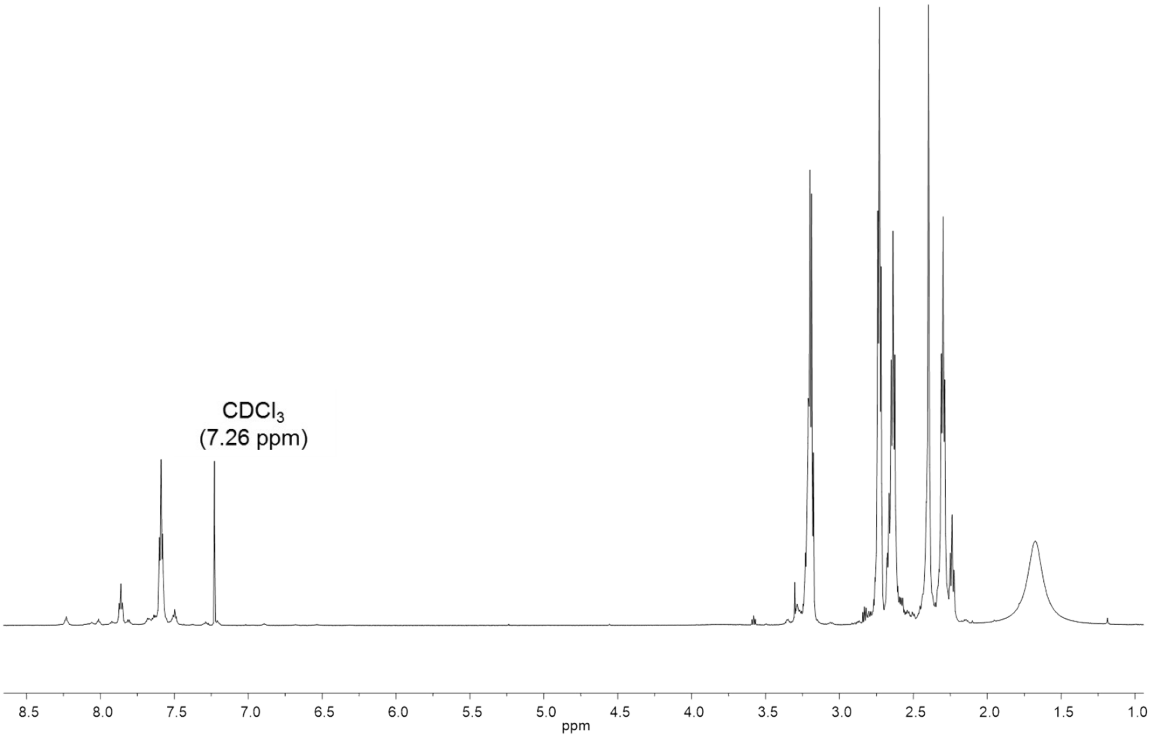

Figure S 18. ^{1}H NMR spectrum ($CDCl_3$) of **5e**.

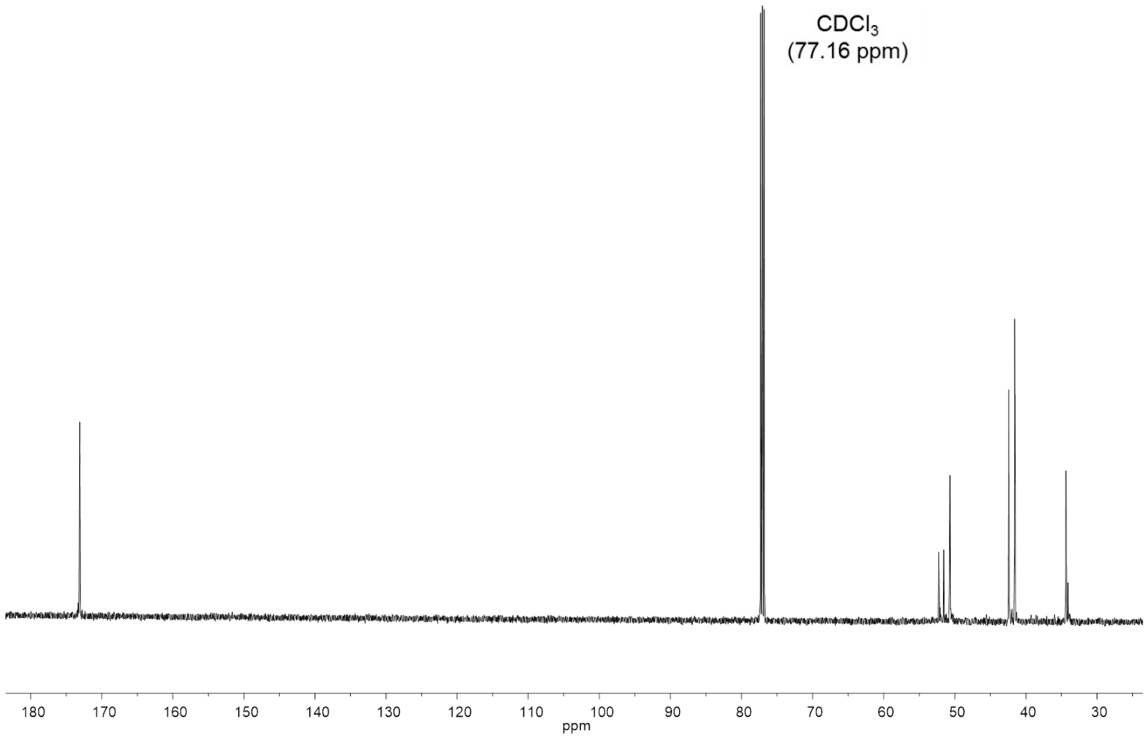

Figure S 19. $^{13}C\{^{1}H\}$ NMR spectrum ($CDCl_3$) of **5e**.

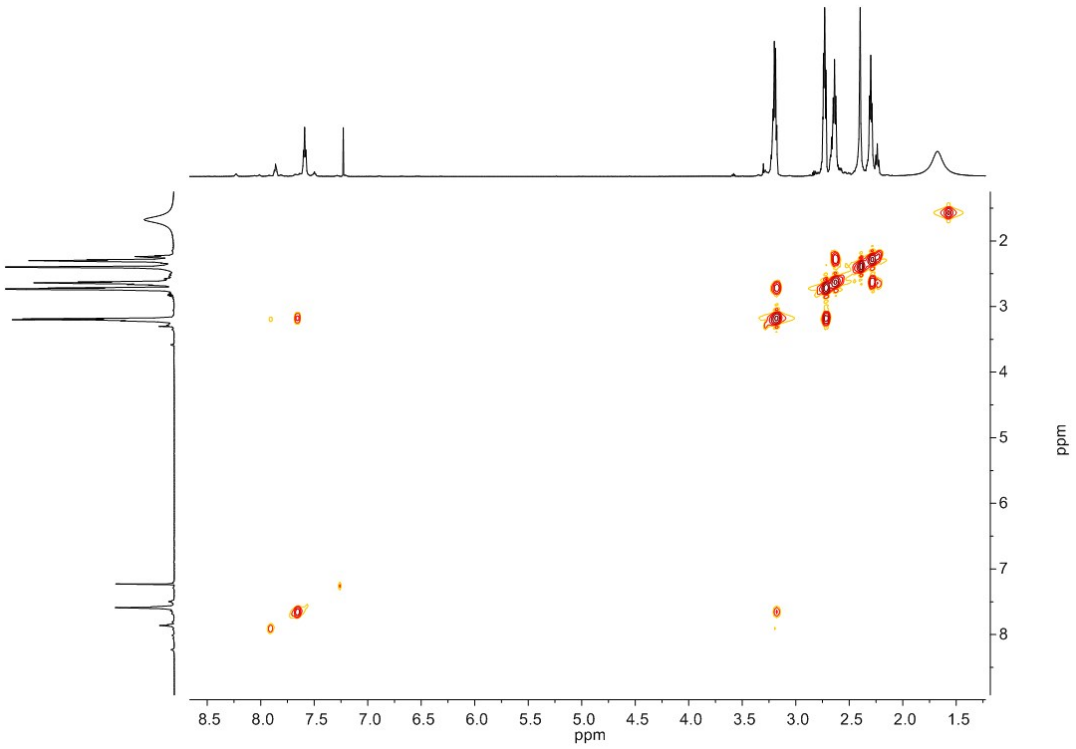

Figure S 20. $^{1}H,^{1}H$-COSYGPSW NMR spectrum ($CDCl_3$) of **5e**.

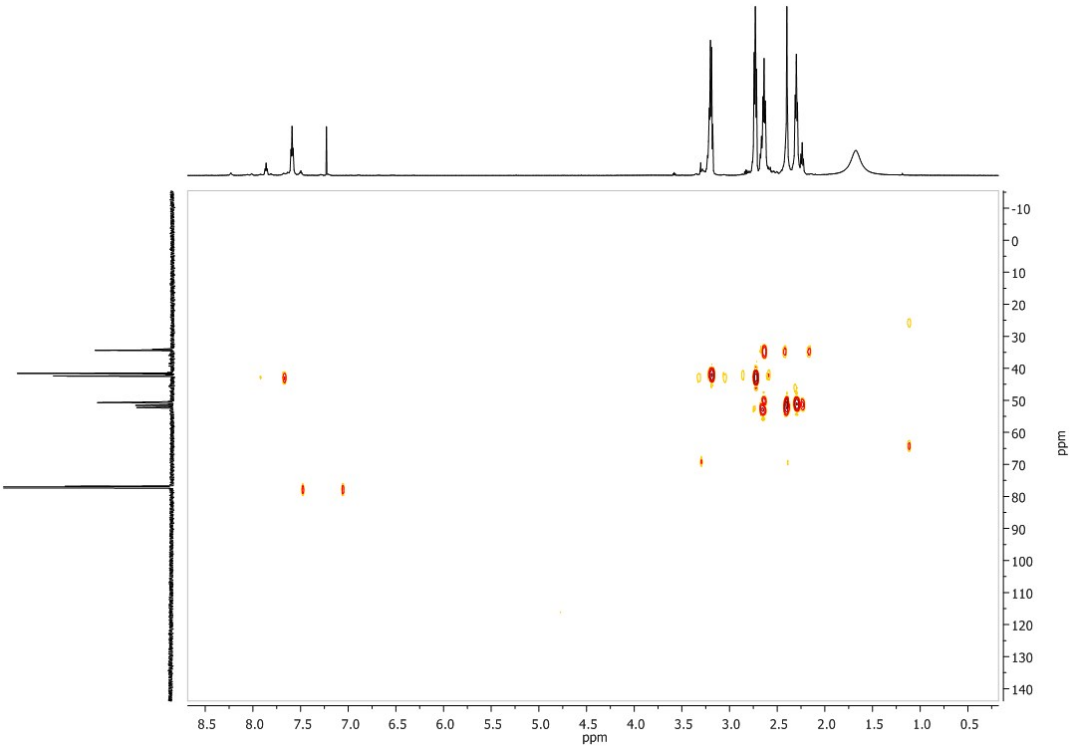

Figure S 21. $^{1}H,^{13}C$-HMBCGP NMR spectrum ($CDCl_3$) of **5e**.

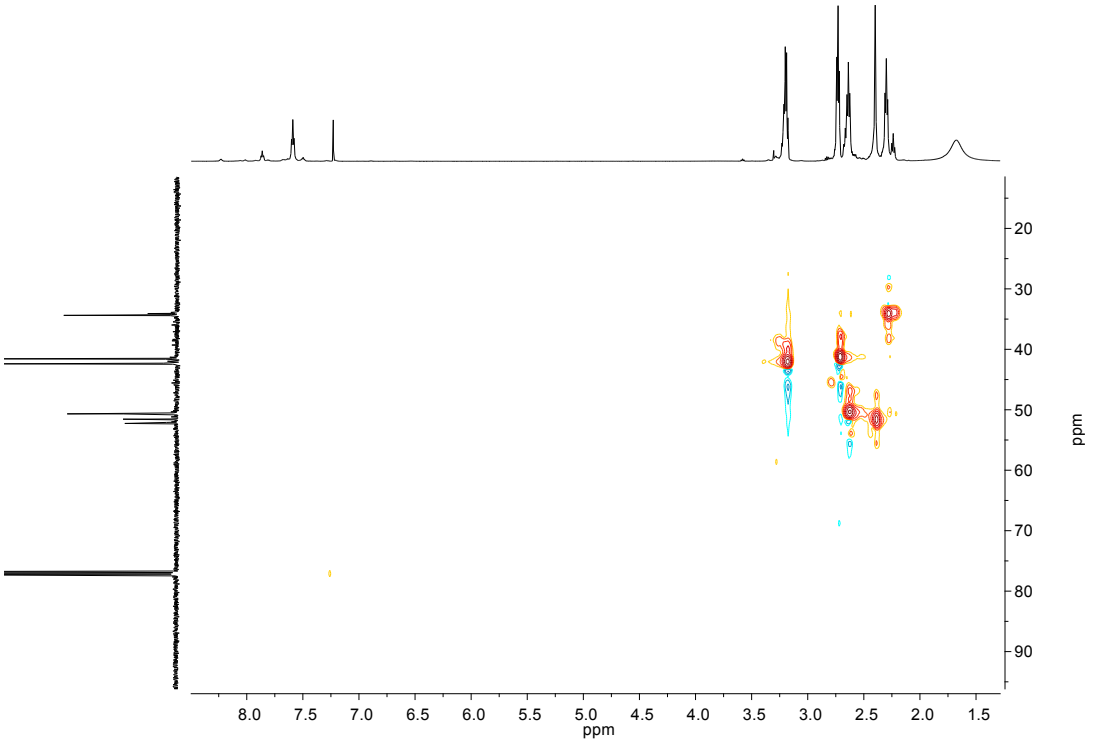

Figure S 22. $^{1}H,^{13}C$-HSQCETGP NMR spectrum ($CDCl_3$) of **5e**.

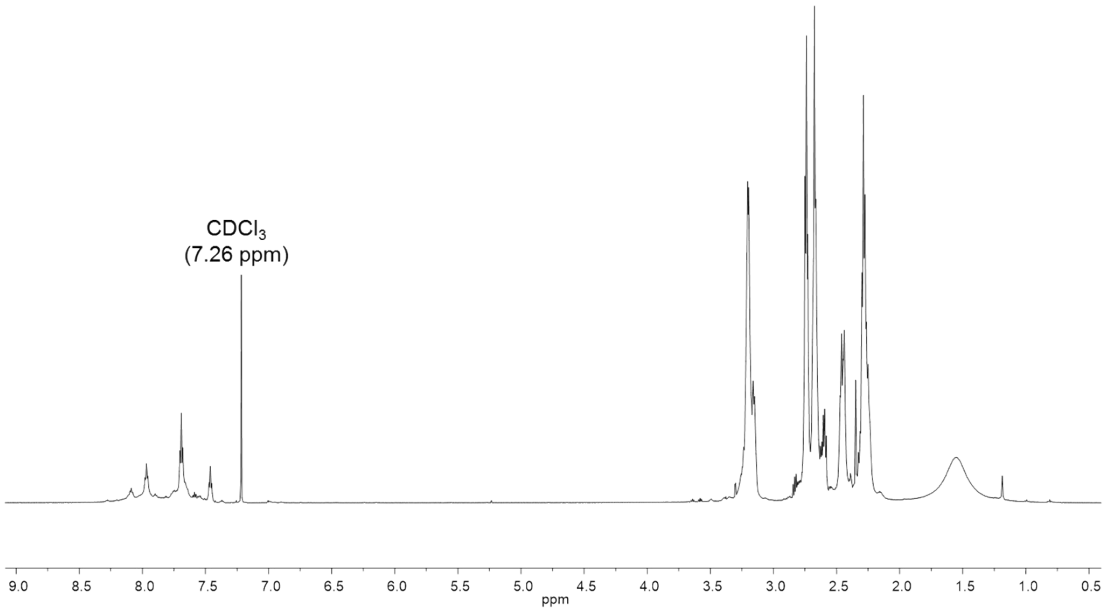

Figure S 23. ^{1}H NMR spectrum ($CDCl_3$) of **5f**.

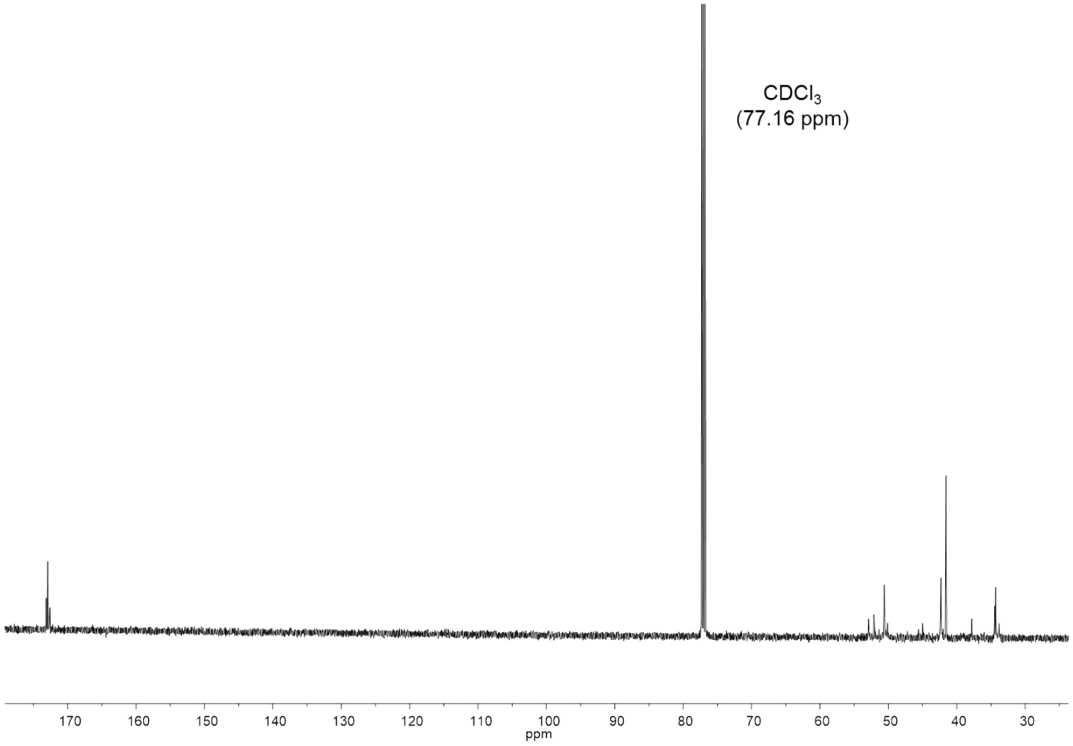

Figure S 24. $^{13}C\{^{1}H\}$ NMR spectrum ($CDCl_3$) of **5f**.

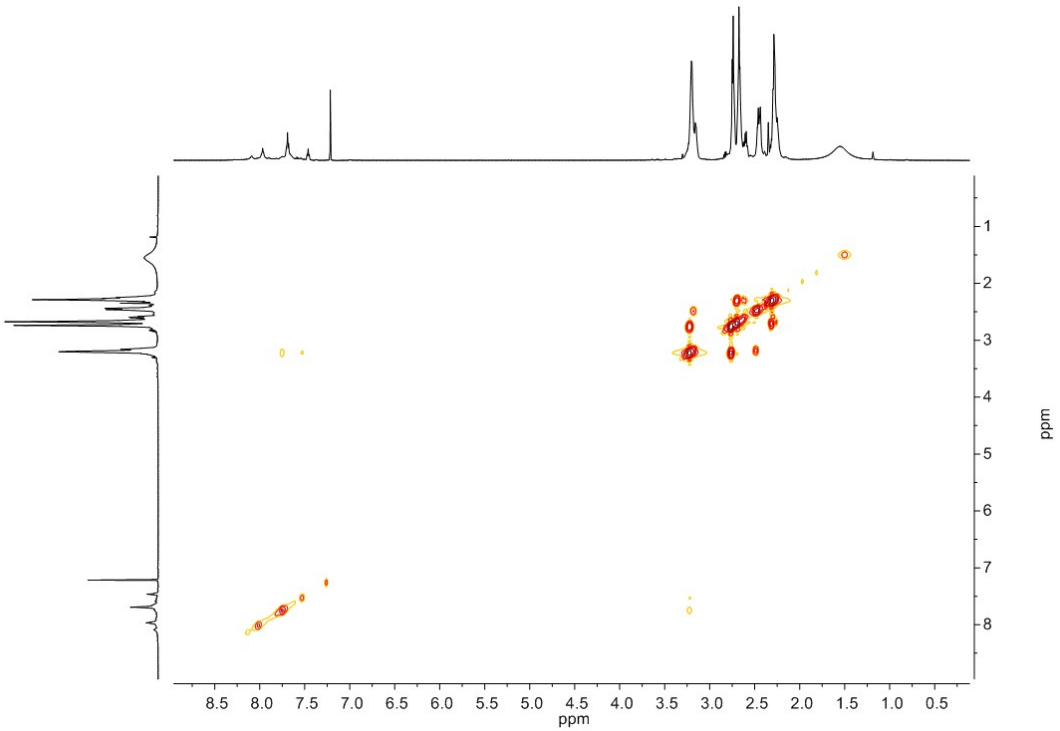

Figure S 25. $^{1}H,^{1}H$-COSYGPSW NMR spectrum ($CDCl_3$) of **5f**.

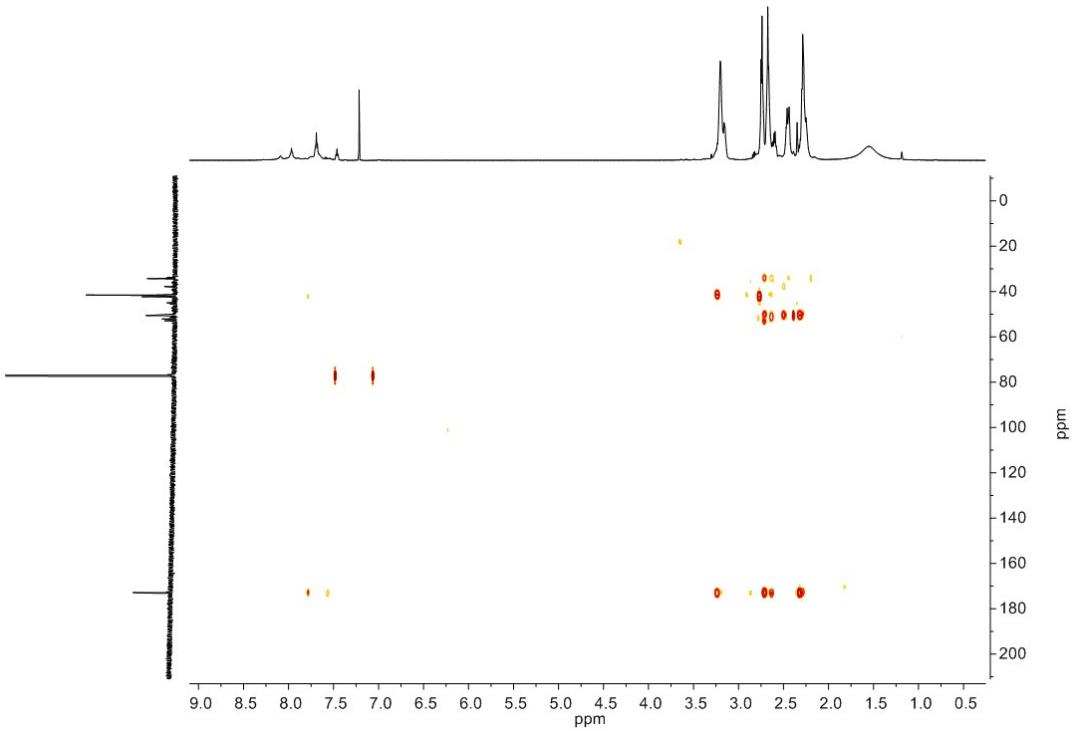

Figure S 26. $^{1}H,^{13}C$-HMBCGP NMR spectrum ($CDCl_3$) of **5f**.

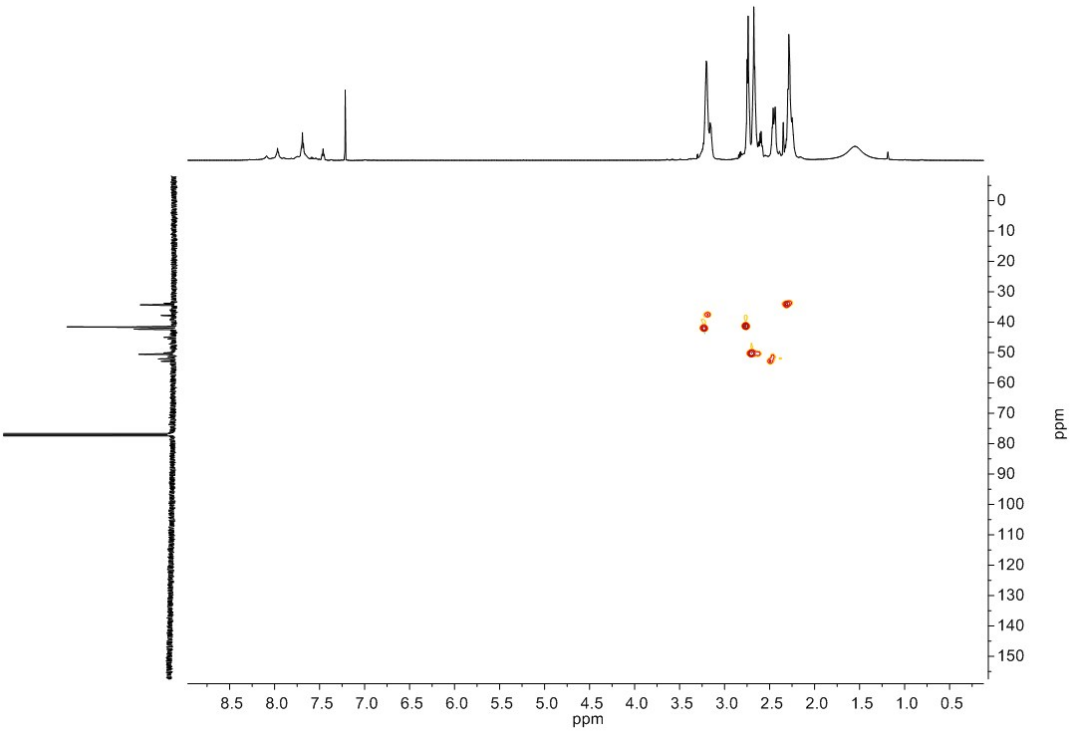

Figure S 27. $^{1}H,^{13}C$-HSQCETGP NMR spectrum ($CDCl_3$) of **5f**.

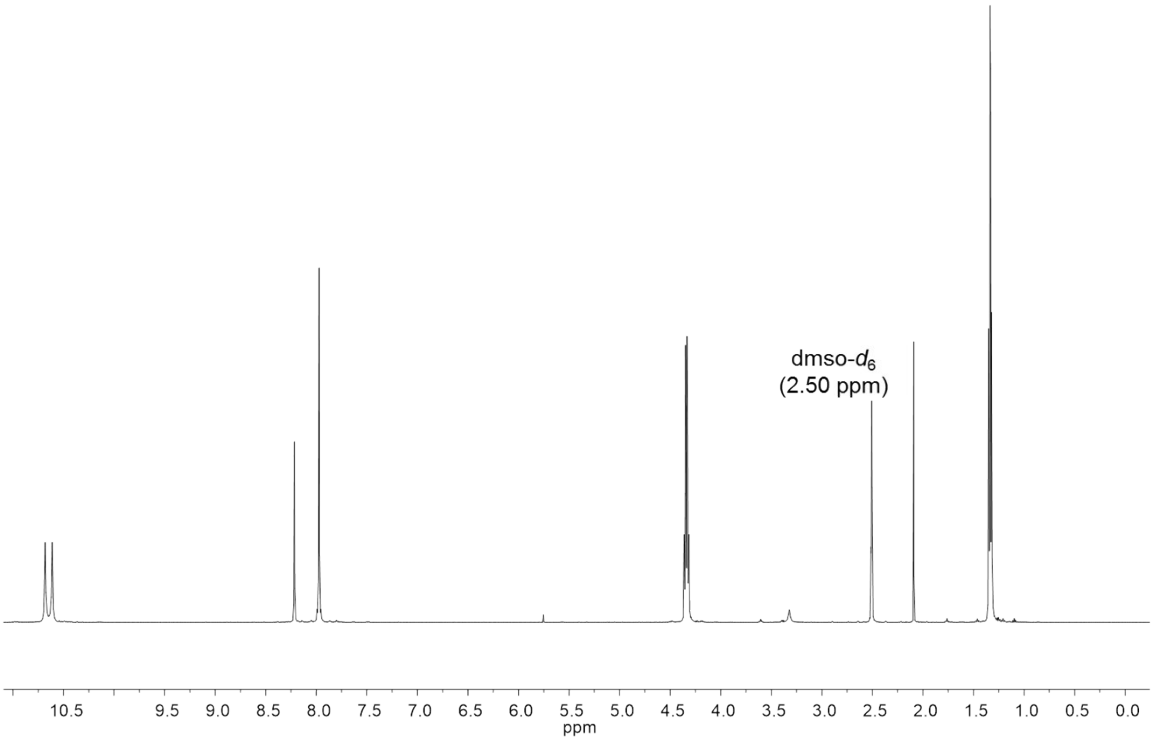

Figure S 28. ^{1}H NMR spectrum (DMSO-d_6) of **8**.

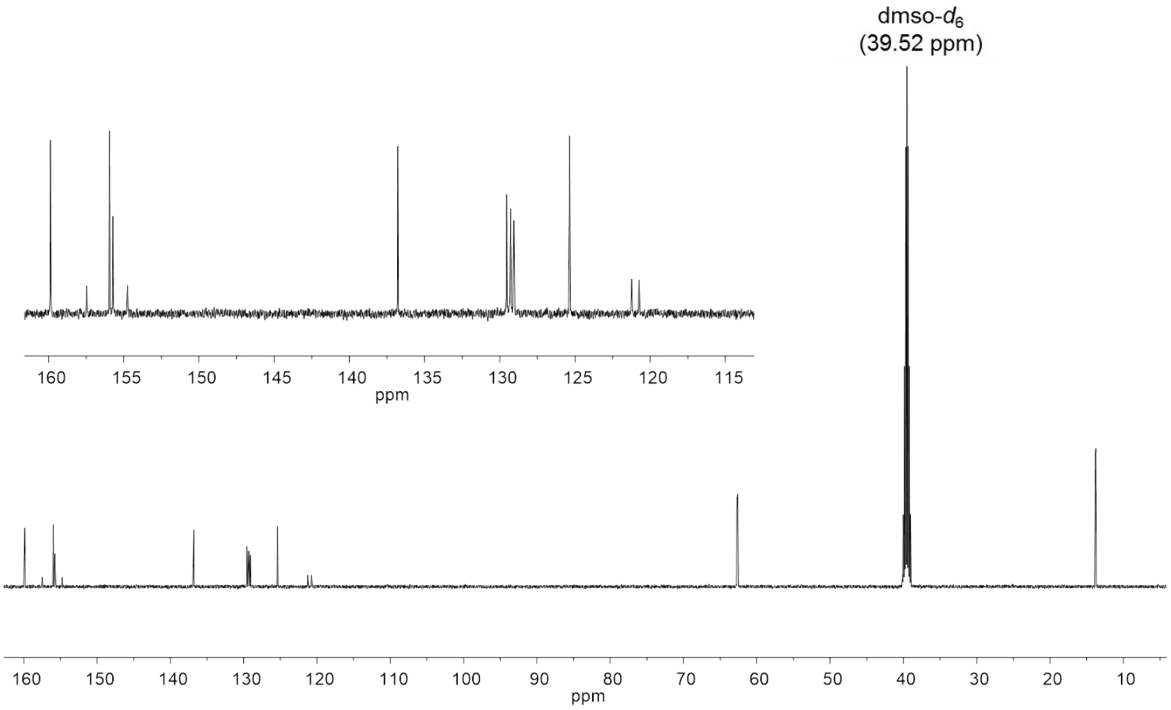

Figure S 29. ^{13}C NMR spectrum (DMSO-d_6) of **8**

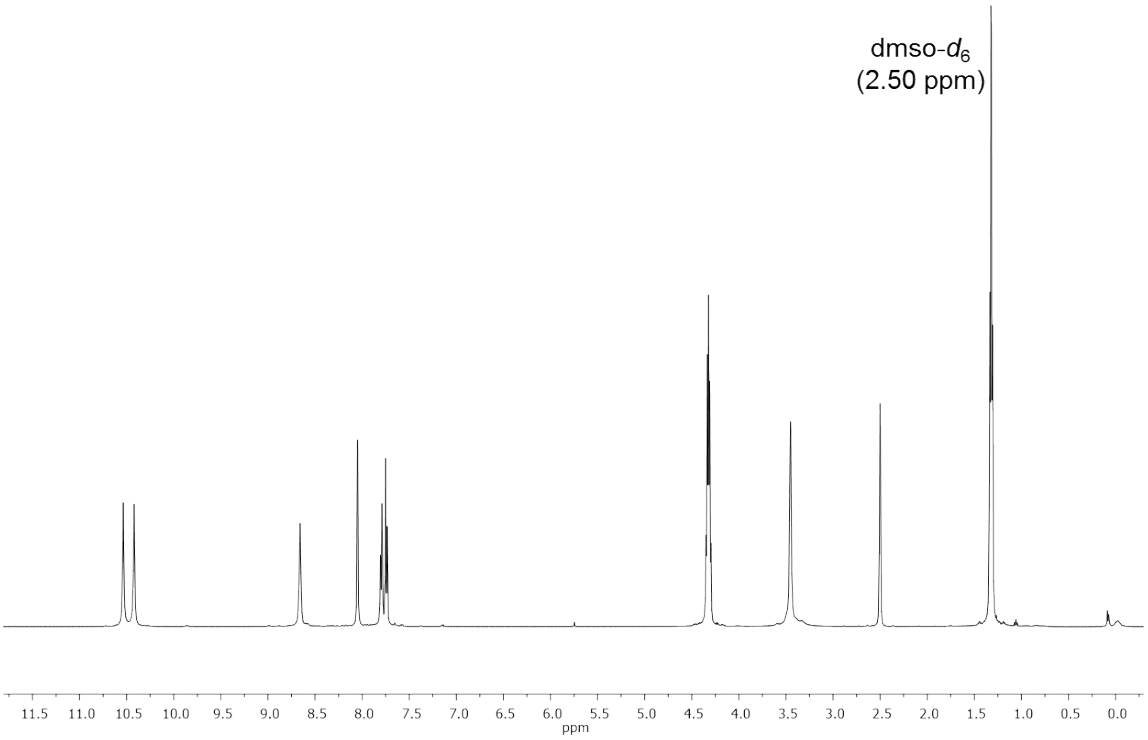

Figure S 30. ^{1}H NMR spectrum (DMSO-d_6) of **7c**.

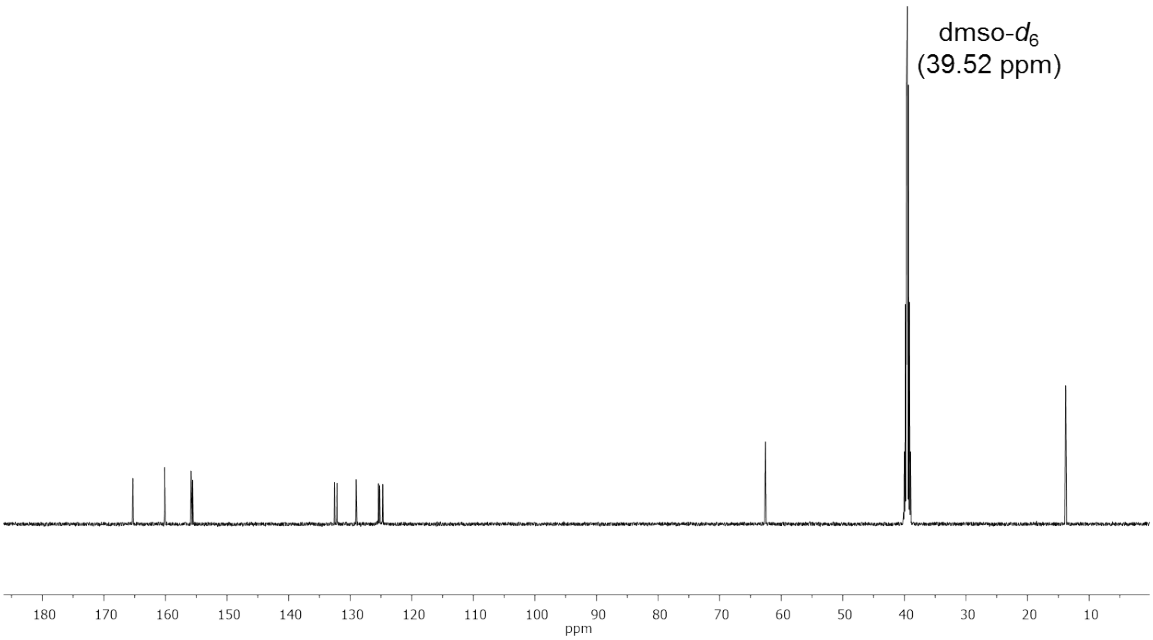

Figure S 31. ^{13}C NMR spectrum (DMSO-d_6) of **7c**.

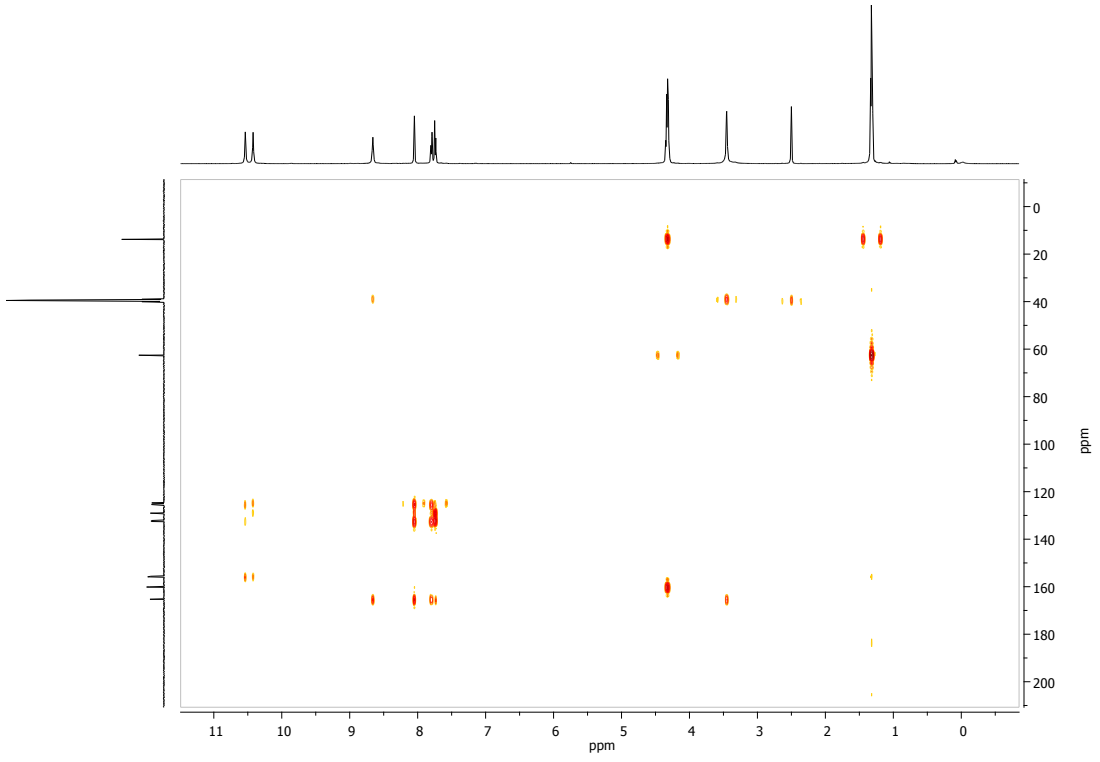

Figure S 32. ^{1}H,^{13}C-HMBCGP NMR spectrum (DMSO-d_6) of **7c**.

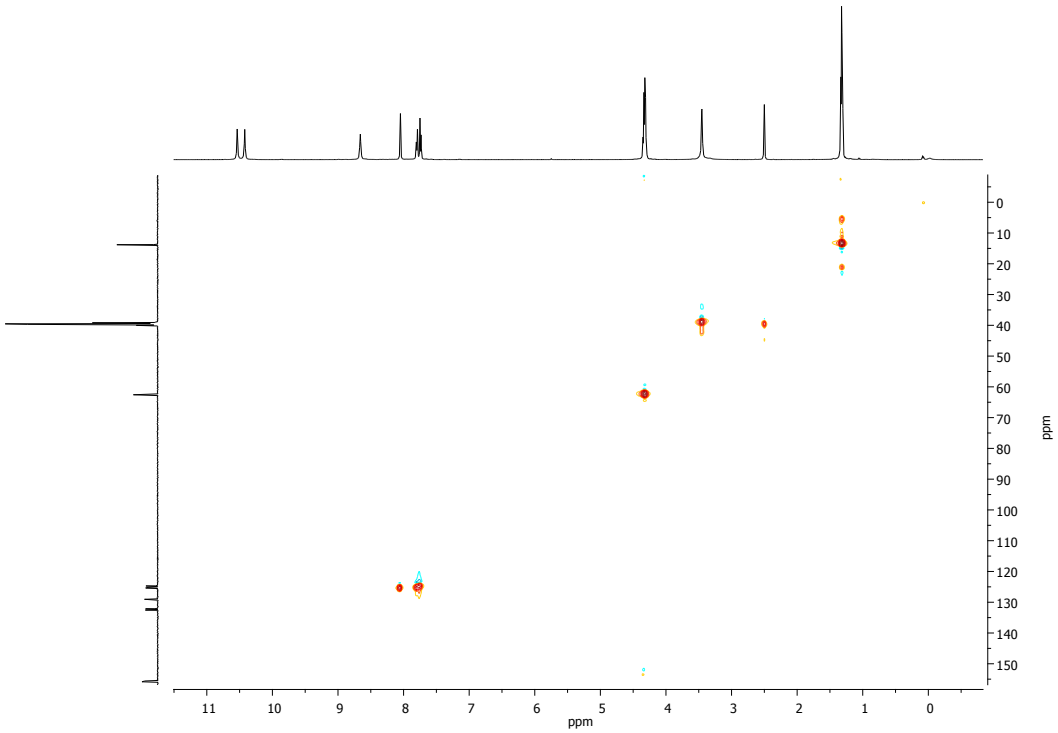

Figure S 33. $^{1}H,^{13}C$-HSQCETGP NMR spectrum (DMSO-d_6) of **7c**.

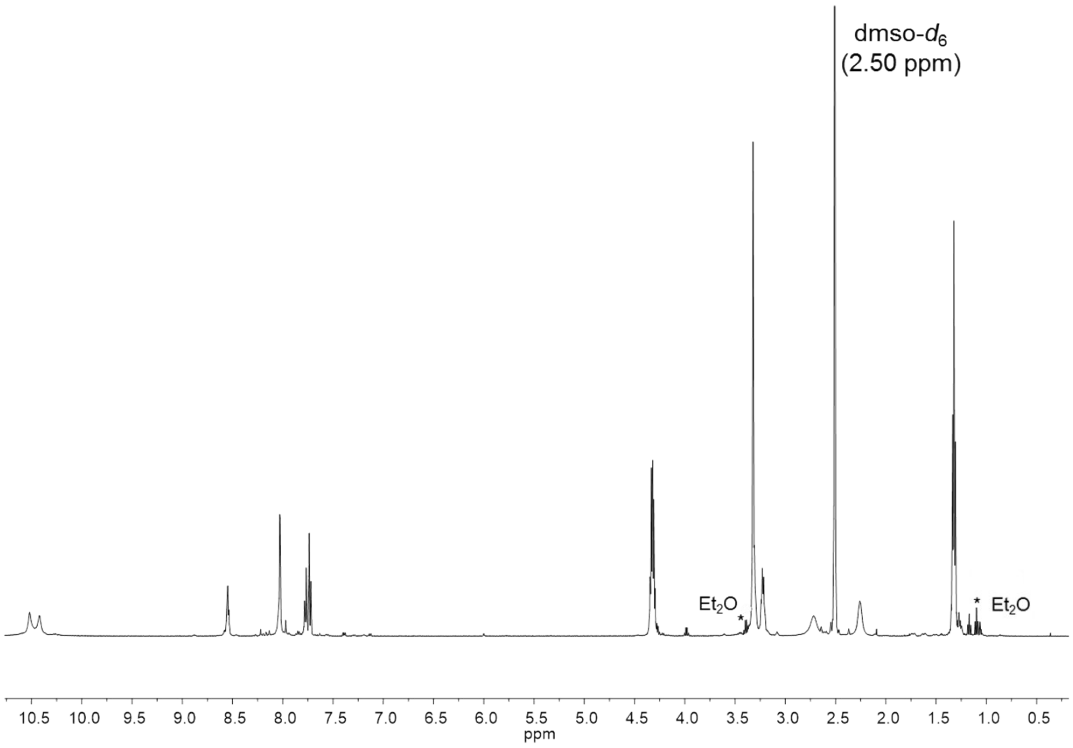

Figure S 34. ^{1}H NMR spectrum (DMSO-d_6) of **7d**.

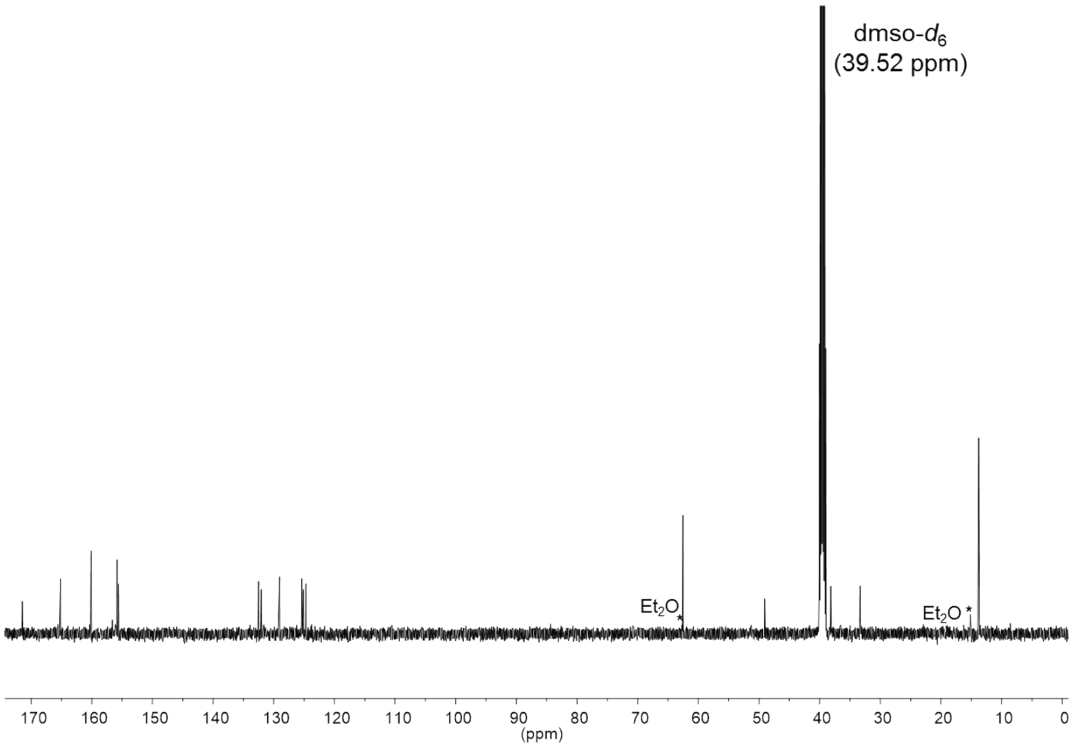

Figure S 35. $^{13}C\{^1H\}$ NMR spectrum (DMSO-d_6) of **7d**.

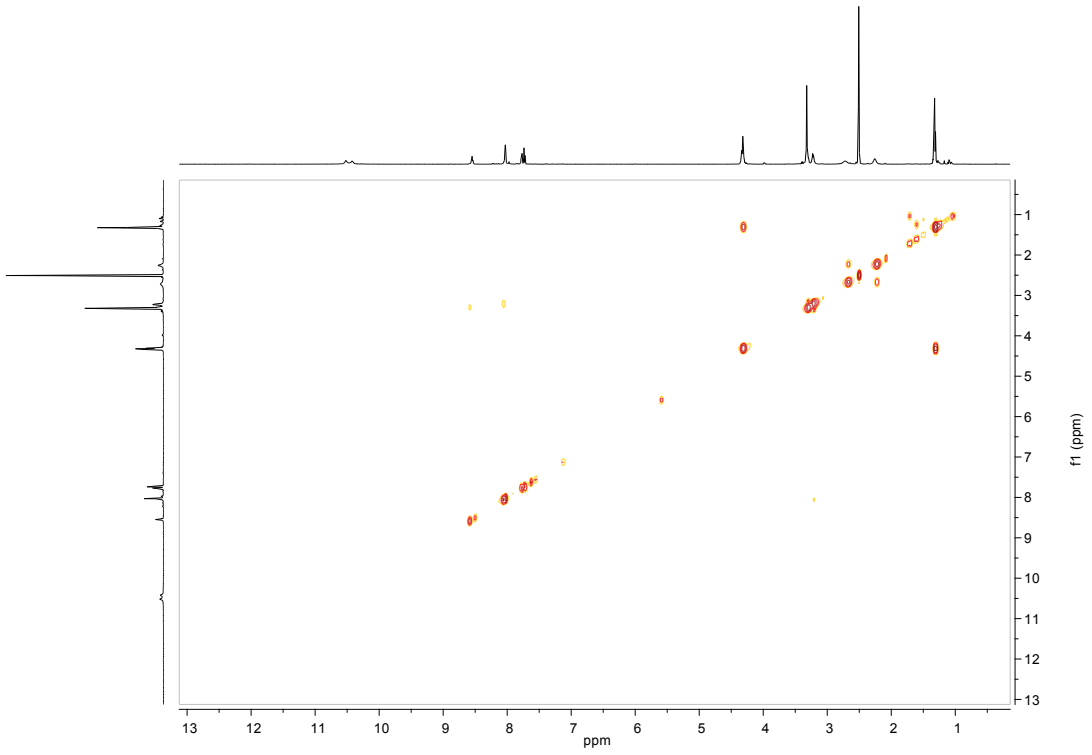

Figure S 36. $^1H,^1H$-COSYGPSW NMR spectrum (DMSO-d_6) of **7d**.

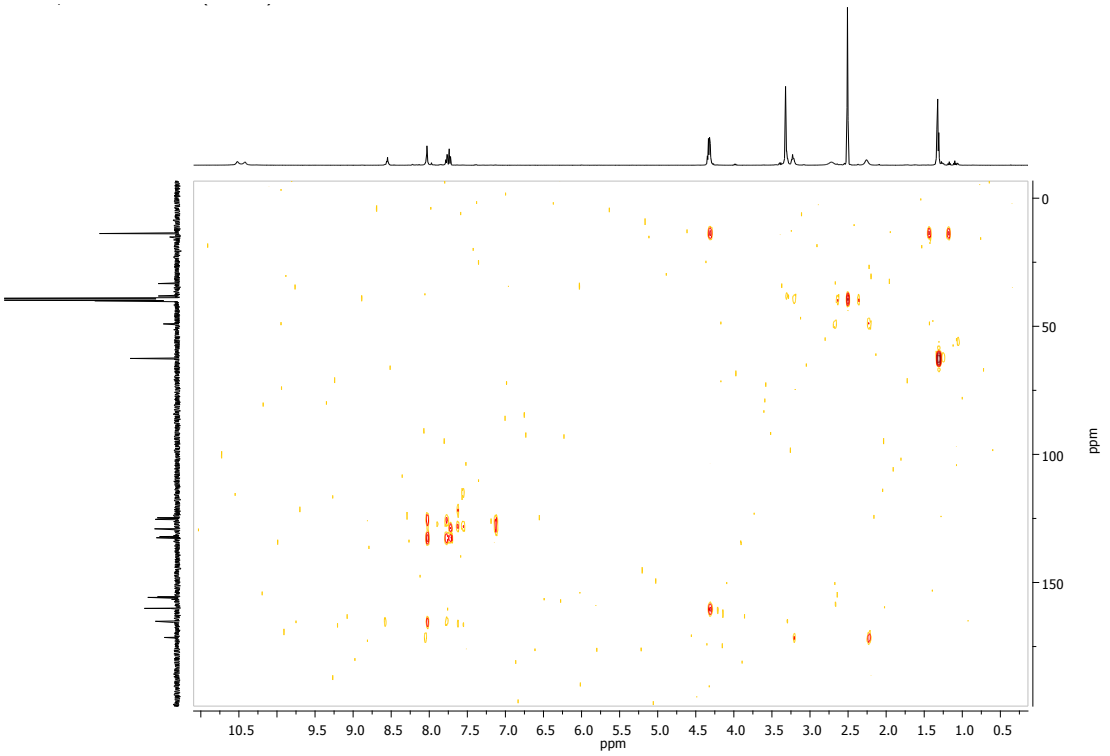

Figure S 37. $^{1}H,^{13}C$-HMBCGP NMR spectrum (DMSO-d_6) of **7d**.

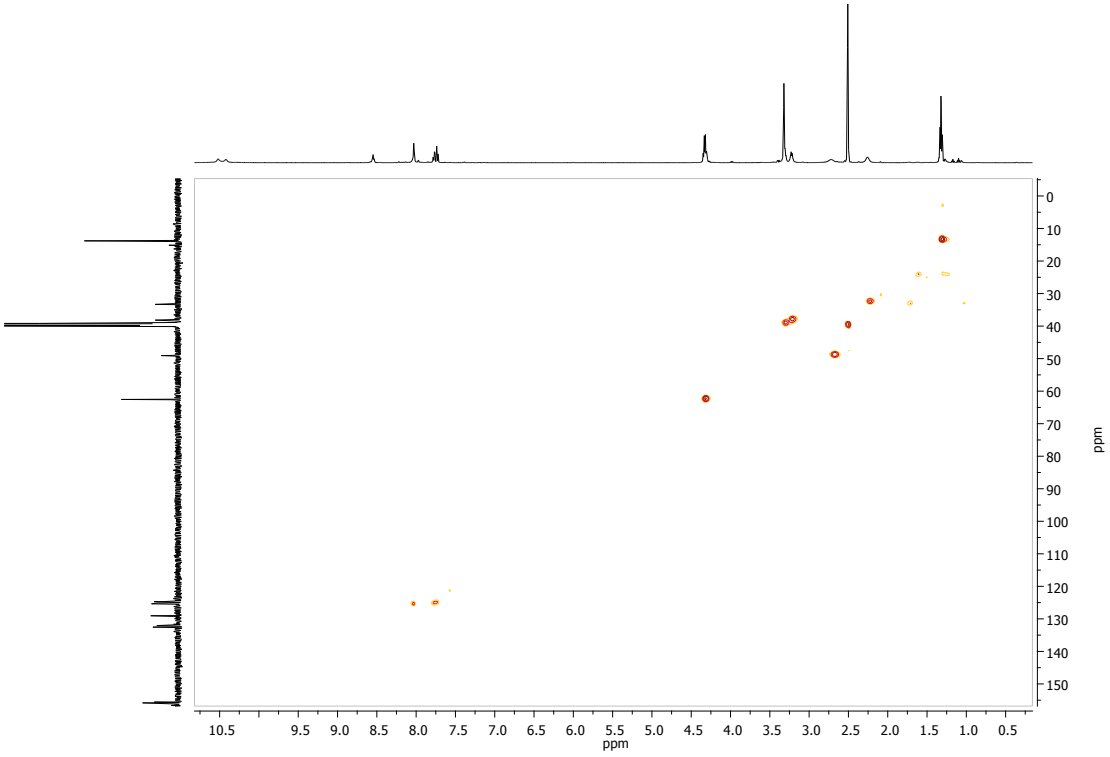

Figure S 38. $^{1}H,^{13}C$-HSQCETGP NMR spectrum (DMSO-d_6) of **7d**.

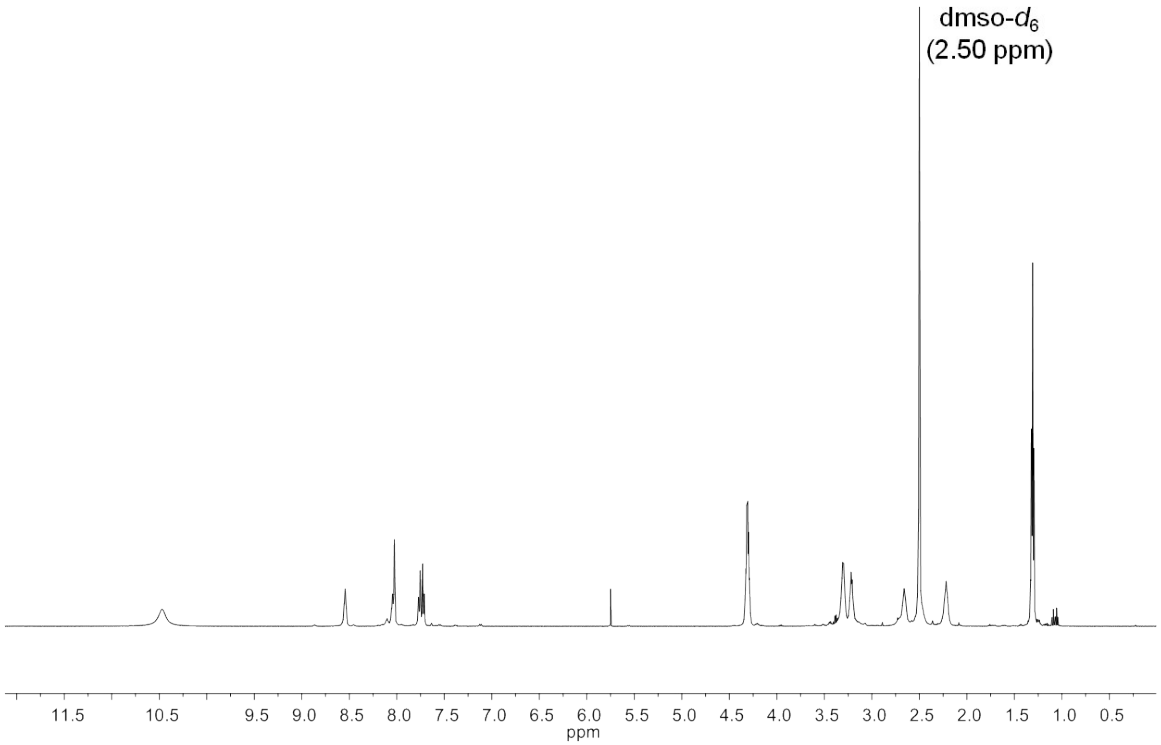

Figure S 39. ^{1}H NMR spectrum (DMSO-d_6) of **7e**.

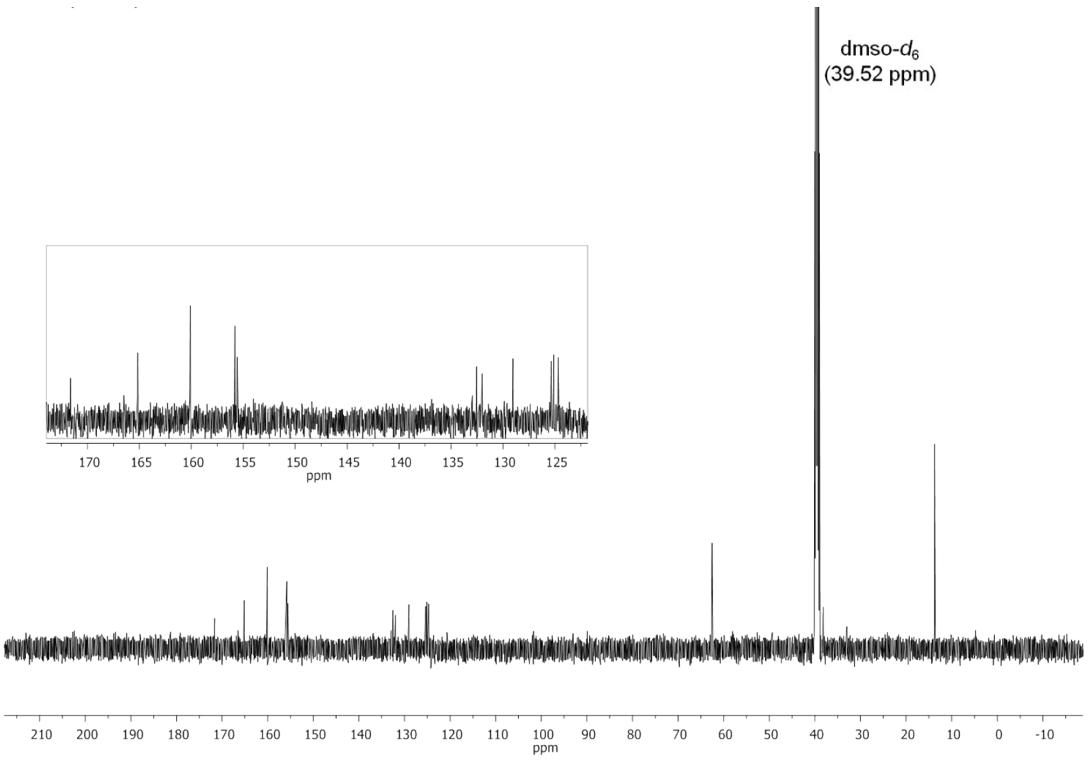

Figure S 40. ^{13}C{^{1}H} NMR spectrum (DMSO-d_6) of **7e**.

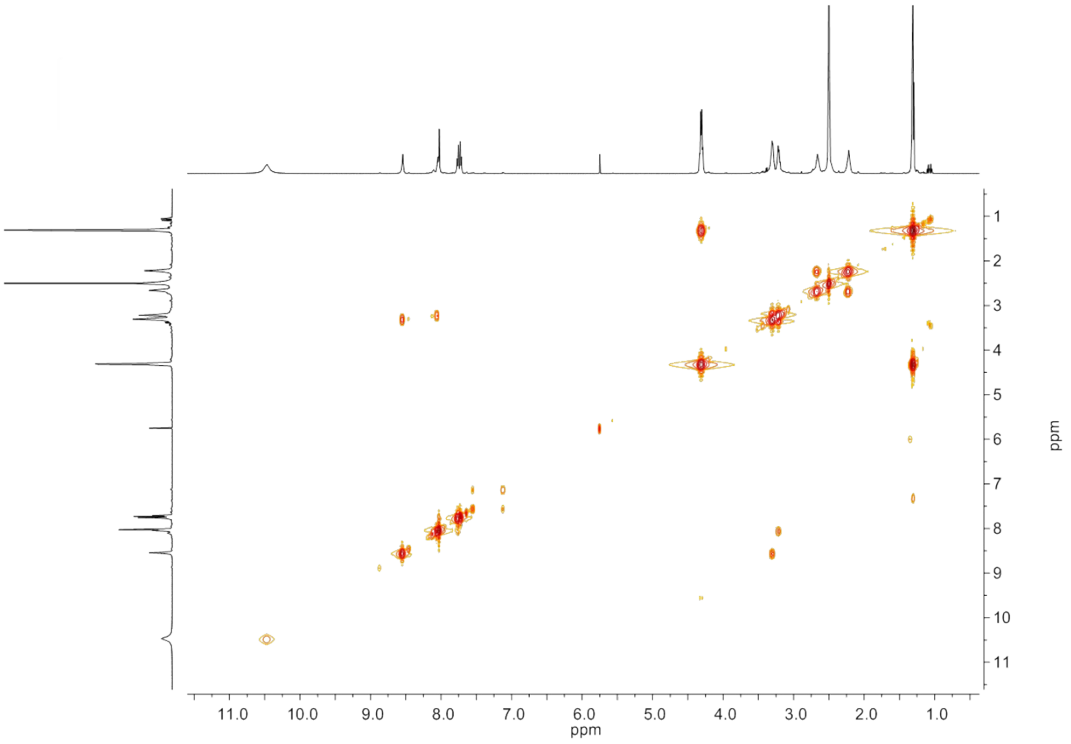

Figure S 41. ^{1}H,^{1}H-COSYGPSW NMR spectrum (DMSO-d_6) of **7e**.

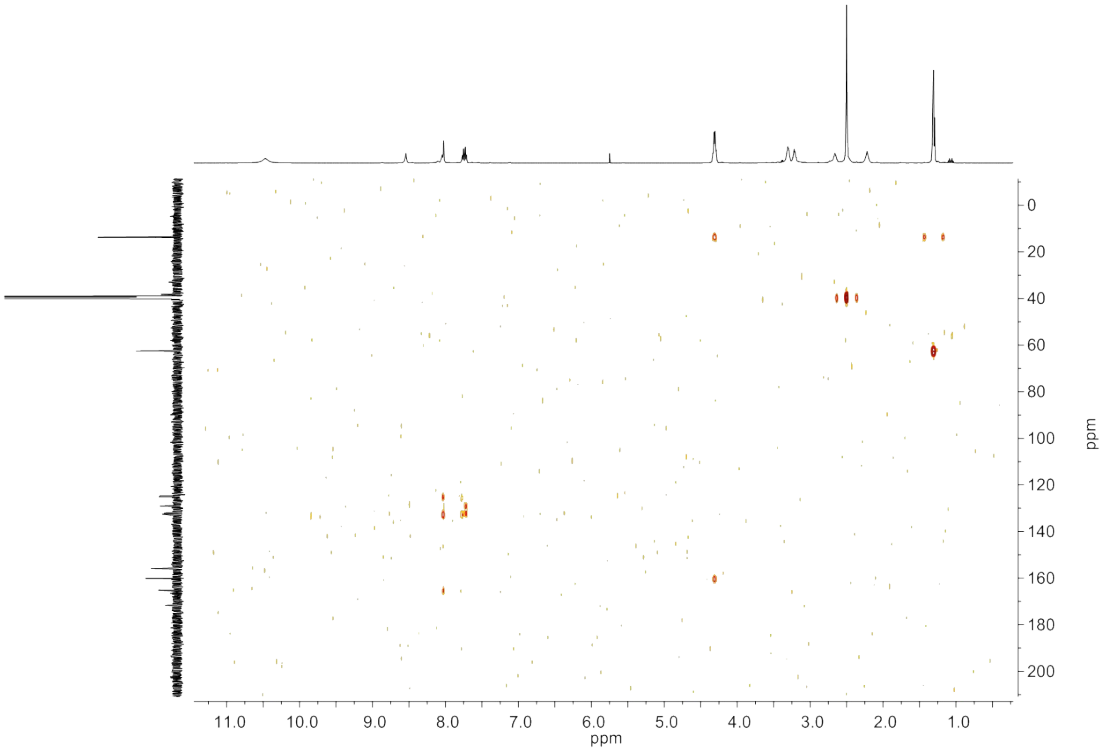

Figure S 42. ^{1}H,^{13}C-HMBCGP NMR spectrum (DMSO-d_6) of **7e**.

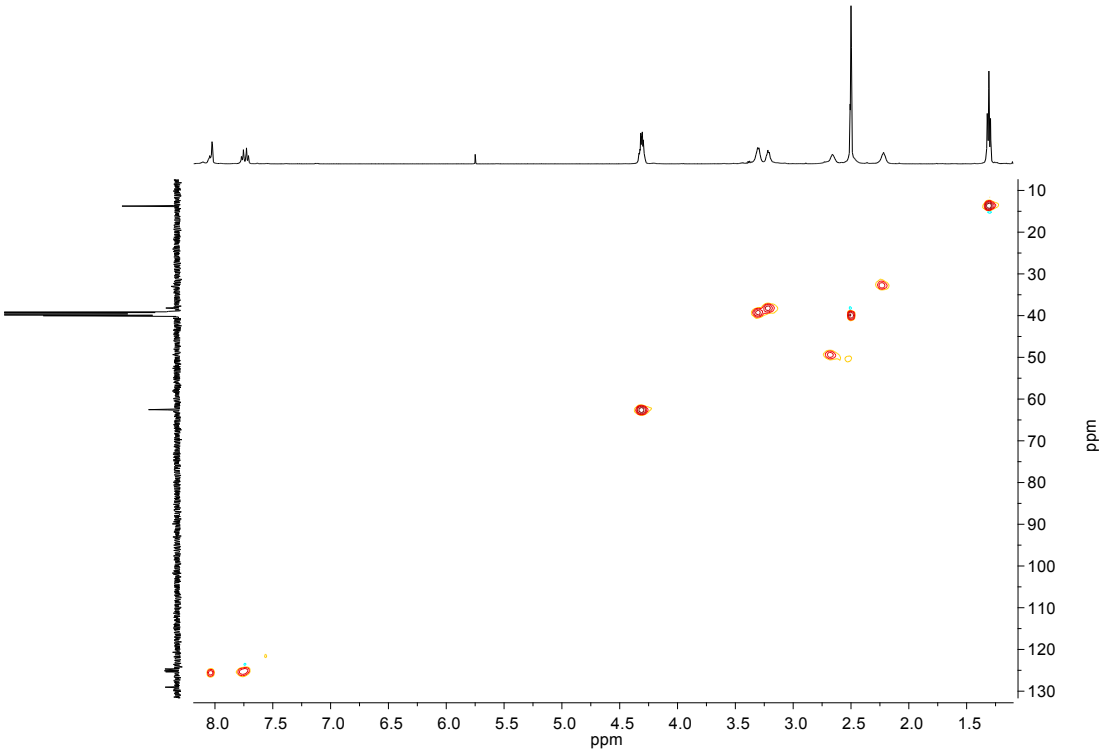

Figure S 43. $^{1}H,^{13}C$-HSQCETGP NMR spectrum (DMSO-d_6) of **7e**.

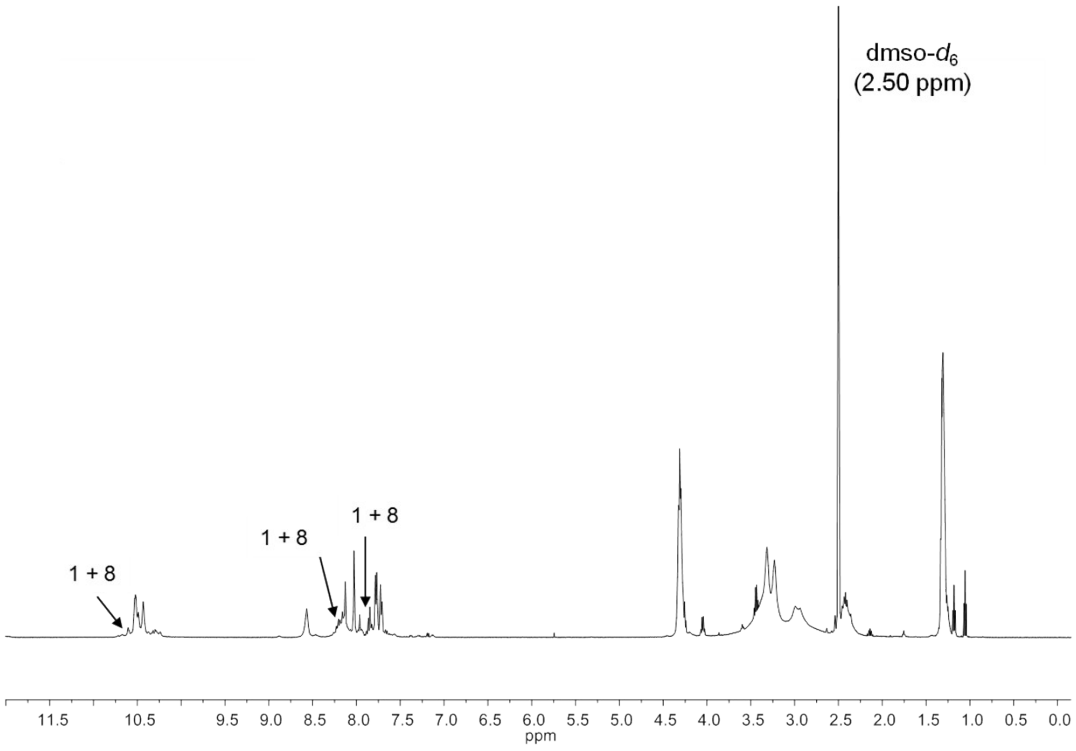

Figure S 44. ^{1}H NMR spectrum (DMSO-d_6) of **7f**. As side products of **7f**, compounds **1** and **8** can be detected of which **1** was formed by hydrolysis out of **8**.[4–6]

4 C. Chen, C. Chien and C. Su, *J. Fluor. Chem.*, 2002, **115**, 75–77.
5 C. A. G. N. Montalbetti and V. Falque, *Tetrahedron*, 2005, **61**, 10827–10852.
6 G. A. Olah, S. J. Kuhn, From Journal of Organic Chemistry, 1961, **1087**, 225-227.

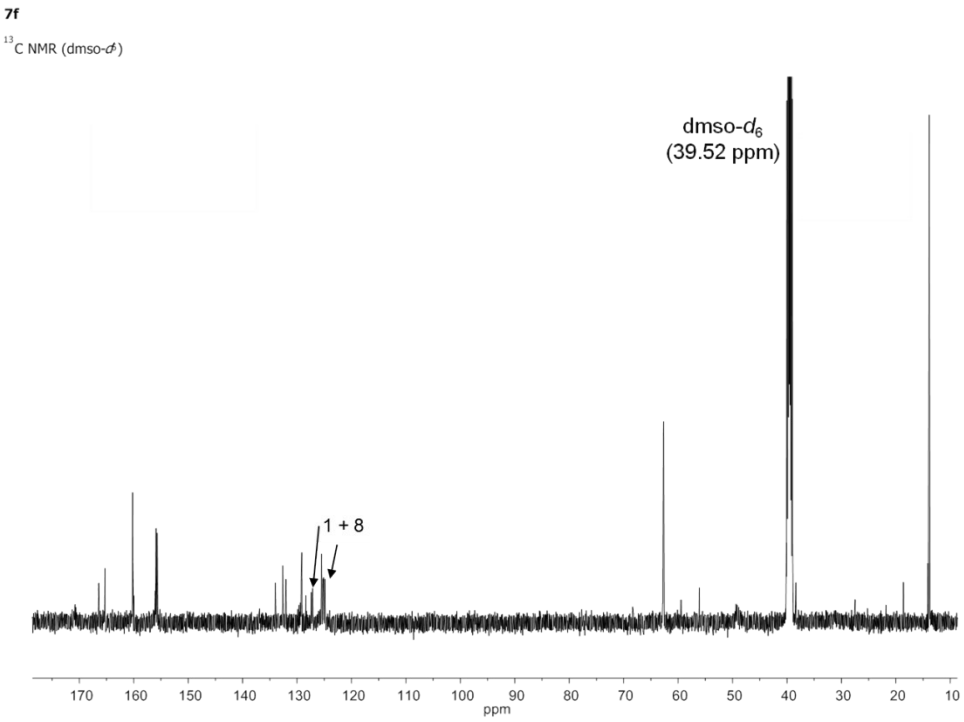

Figure S 45. $^{13}C\{^{1}H\}$ NMR spectrum (DMSO-d_6) of **7f**.

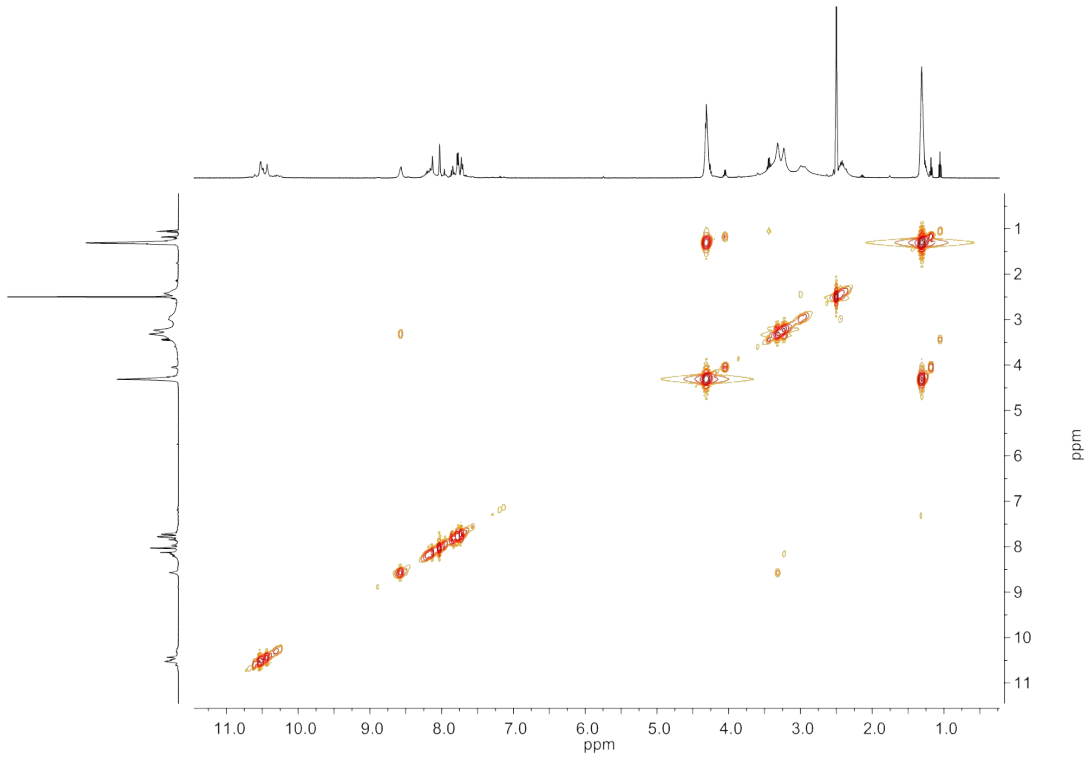

Figure S 46. $^{1}H,^{1}H$-COSYGPSW NMR spectrum (DMSO-d_6) of **7f**.

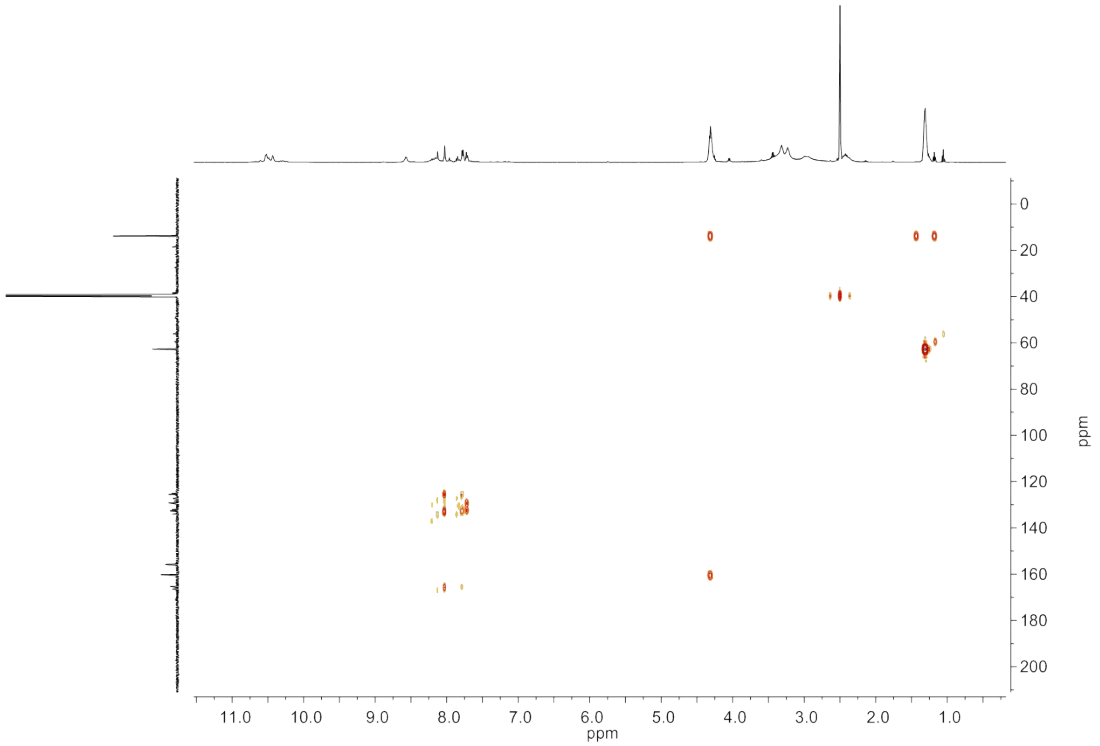

Figure S 47. $^{1}H,^{13}C$-HMBCGP NMR spectrum (DMSO-d_6) of **7f**.

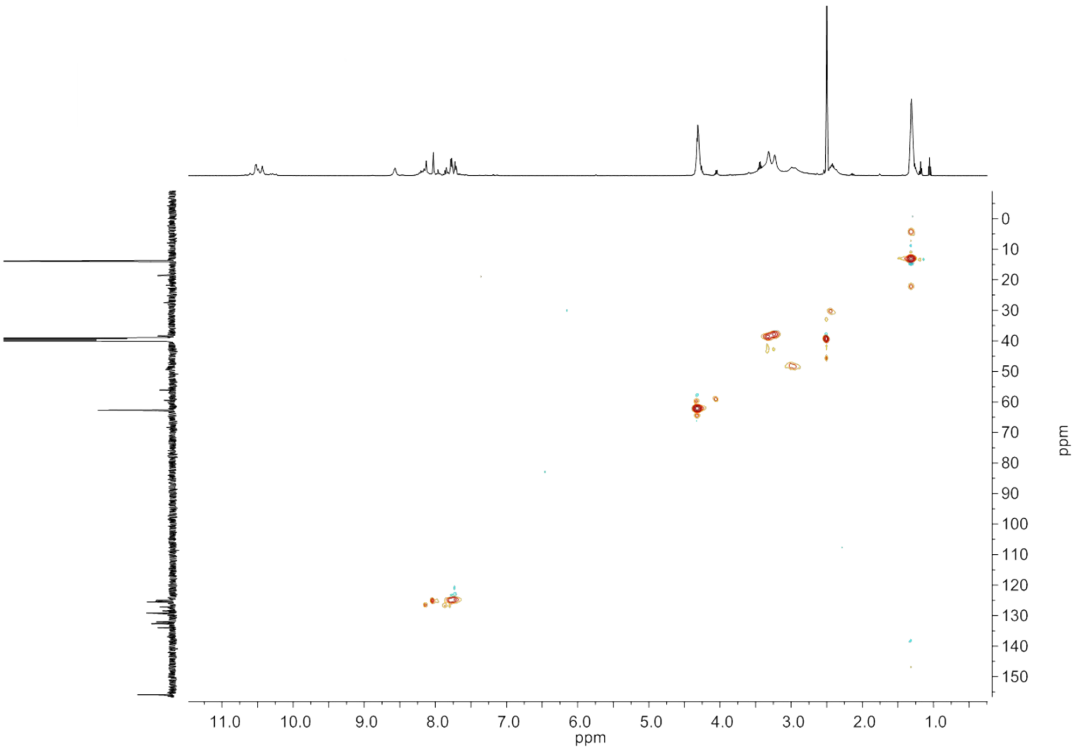

Figure S 48. $^{1}H,^{13}C$-HSQCETGP NMR spectrum (DMSO-d_6) of **7f**.

Preliminary remark: In Figures S49–S62 the ESI-MS spectra of individual compounds are presented. The spectrum on top is the experimental obtained spectrum. The indicated ion peaks are shown underneath with their calculated isotope distribution patterns, starting from the lowest assigned *m*/z value to the highest.

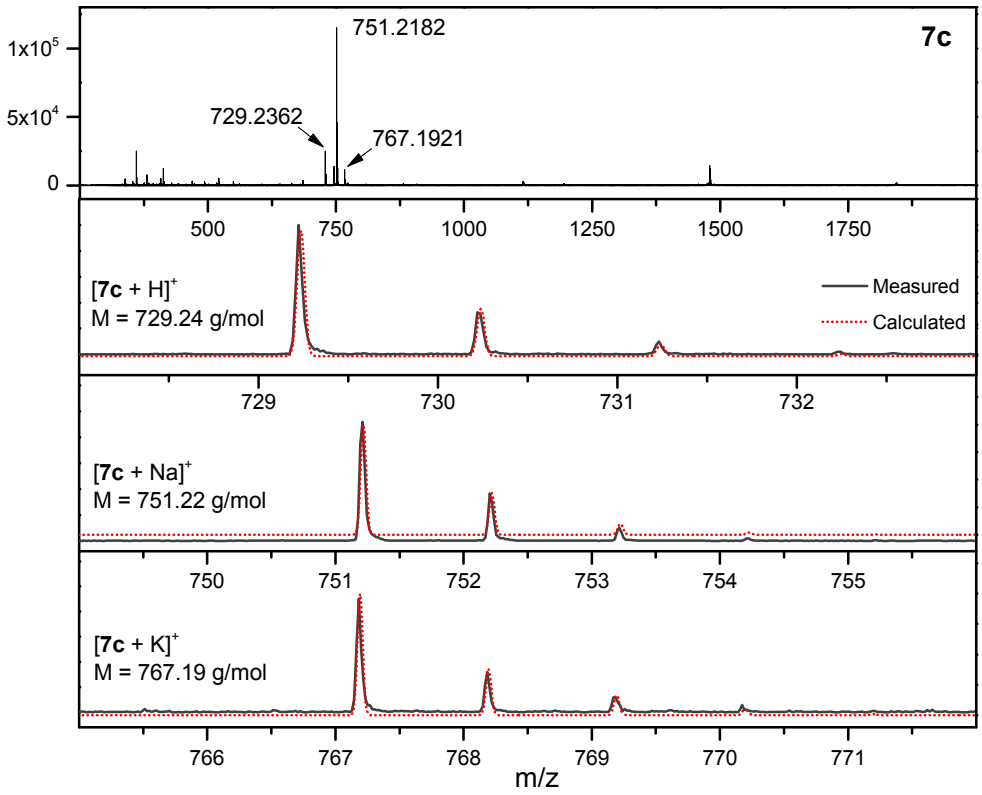

Figure S 49. ESI-MS spectrum of **7c**.

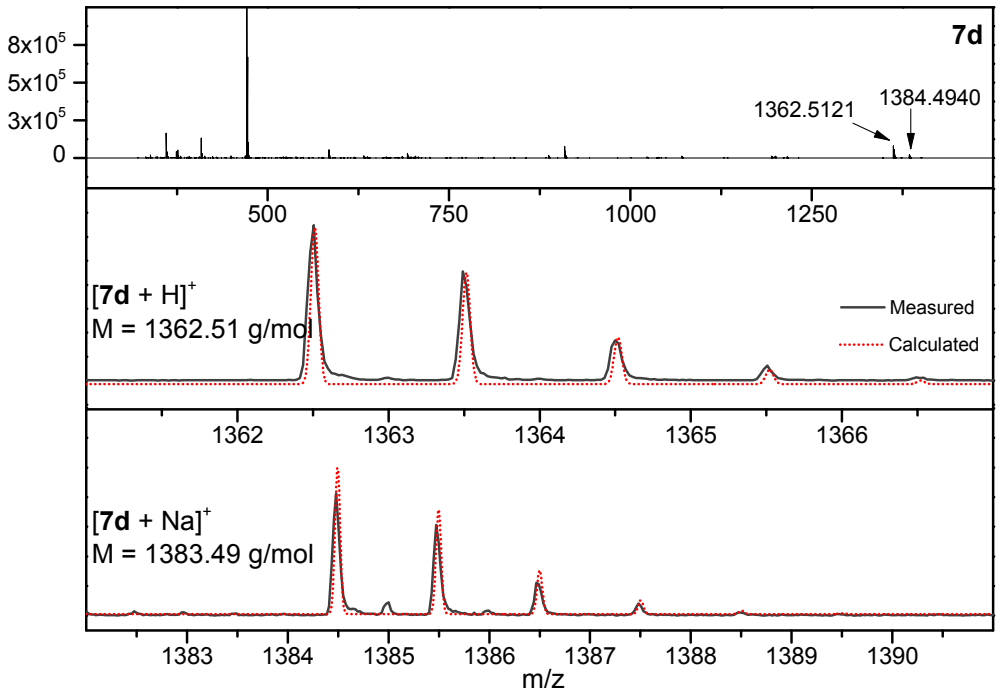

Figure S 50. ESI-MS spectrum of **7d**.

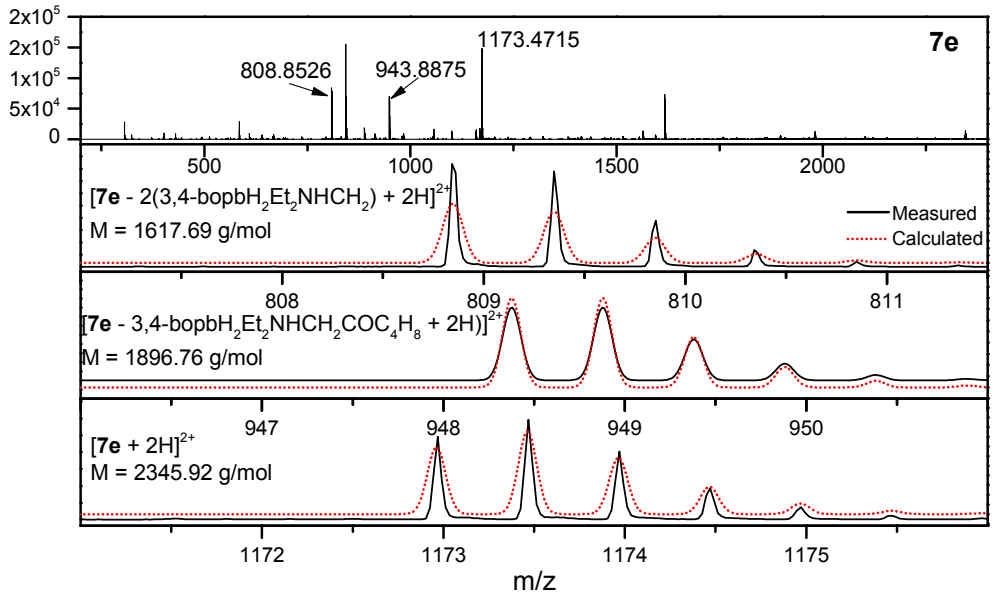

Figure S 51. ESI-MS spectrum of **7e**.

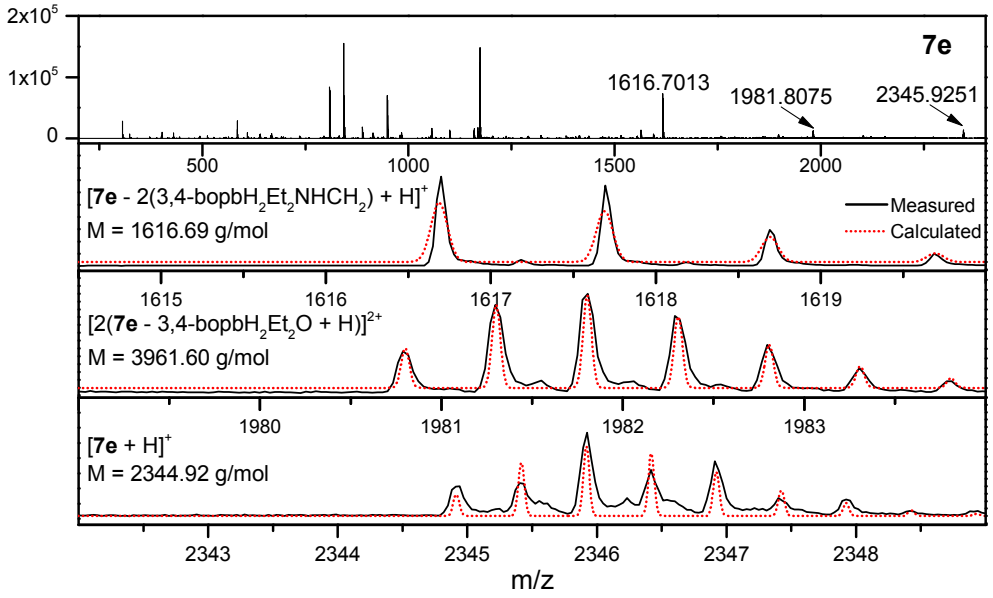

Figure S 52. ESI-MS spectrum of **7e**.

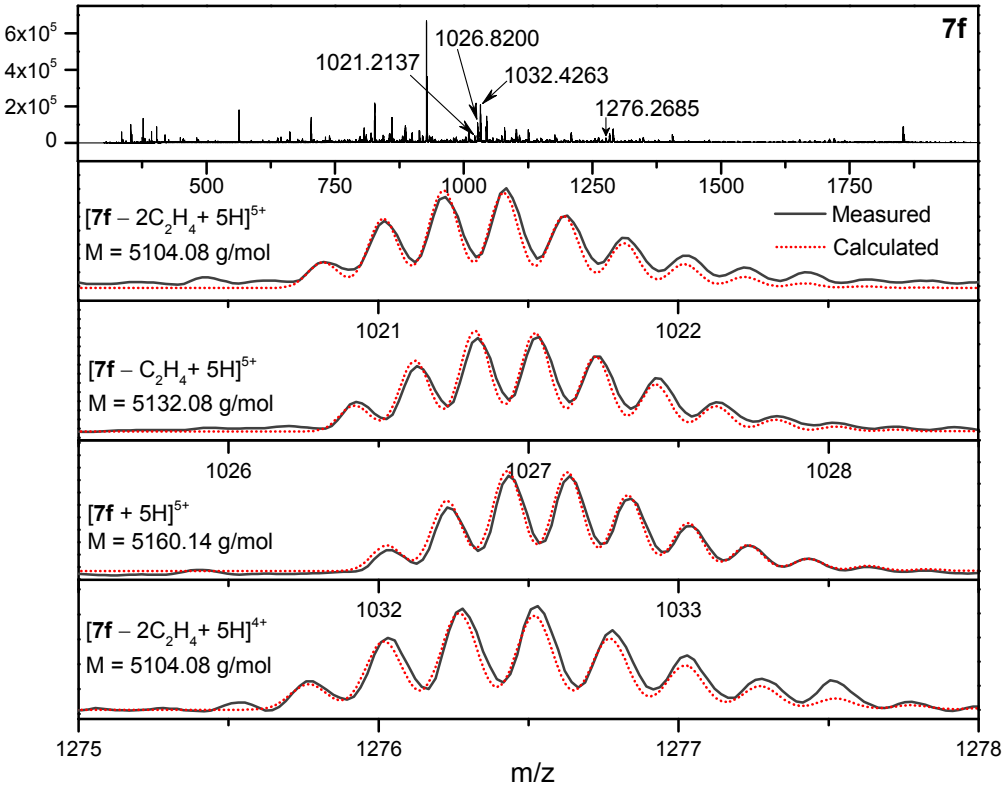

Figure S 53. ESI-MS spectrum of **7f**.

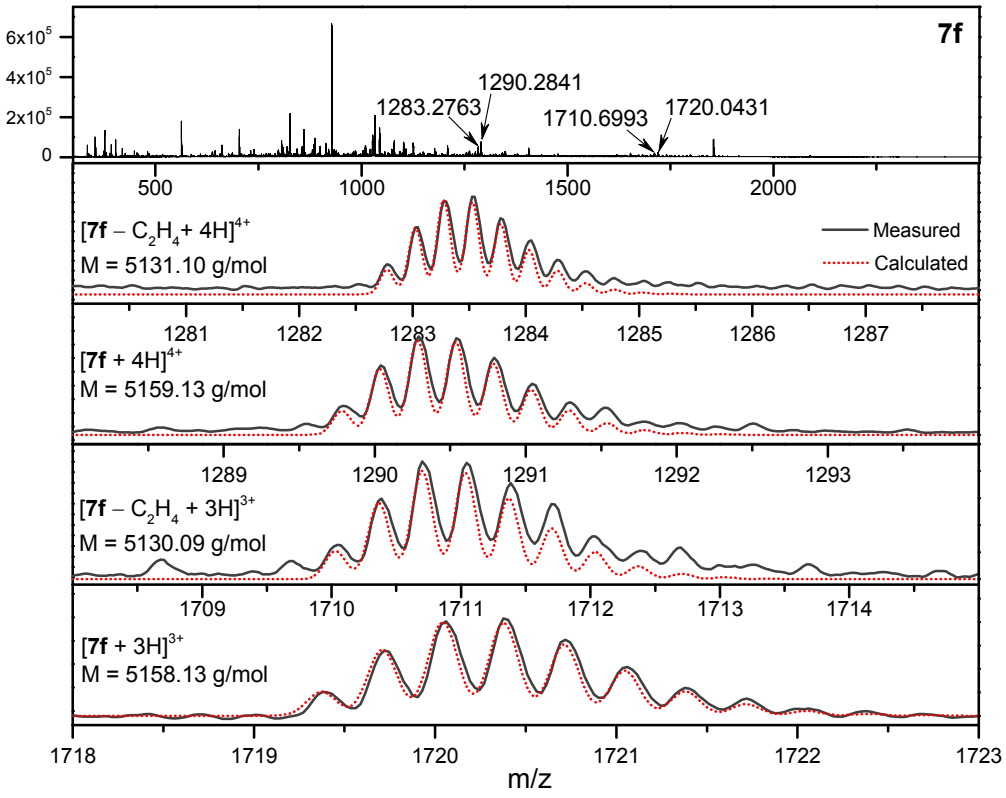

Figure S 54. ESI-MS spectrum of **7f**.

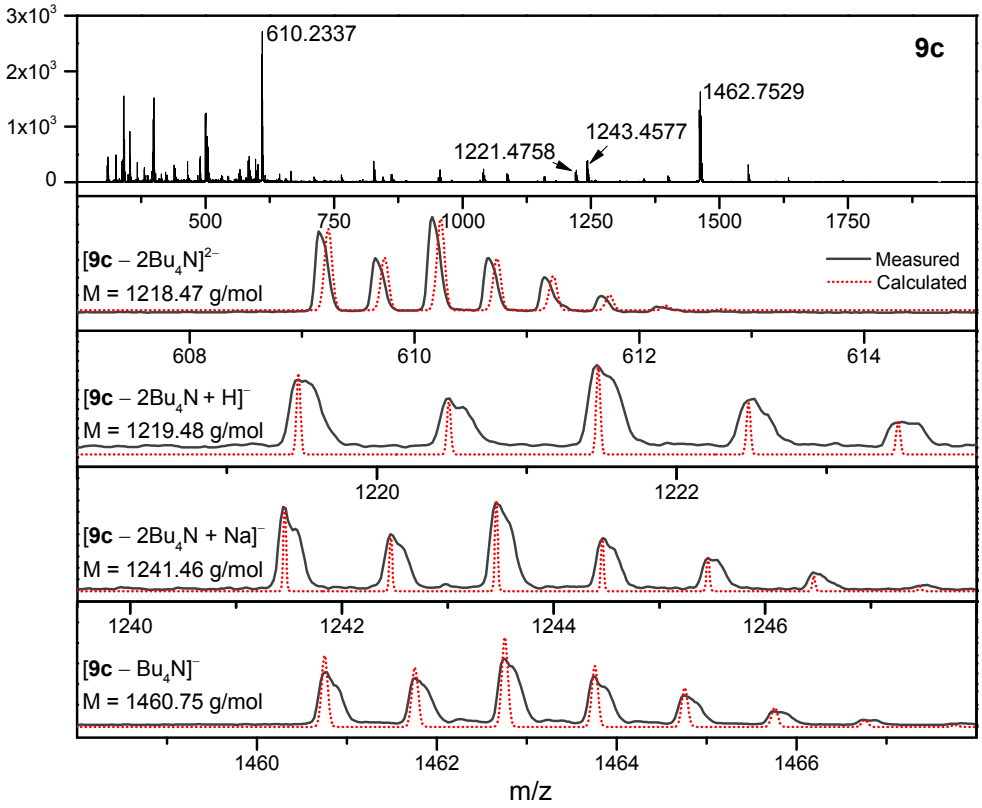

Figure S 55. ESI-MS spectrum of **9c**.

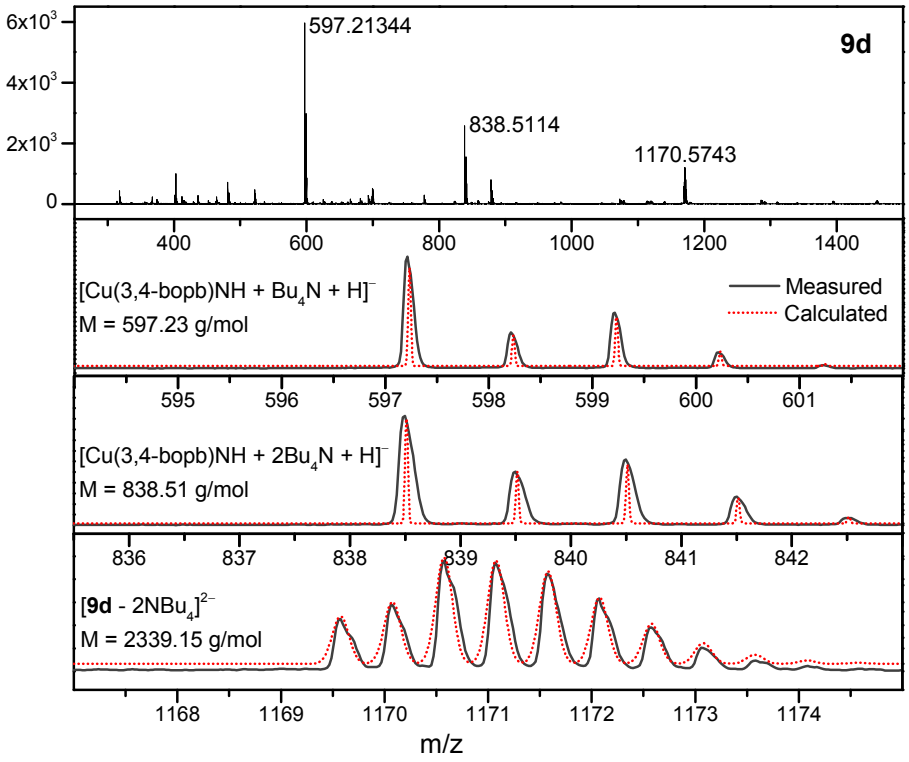

Figure S 56. ESI-MS spectrum of **9d**.

.

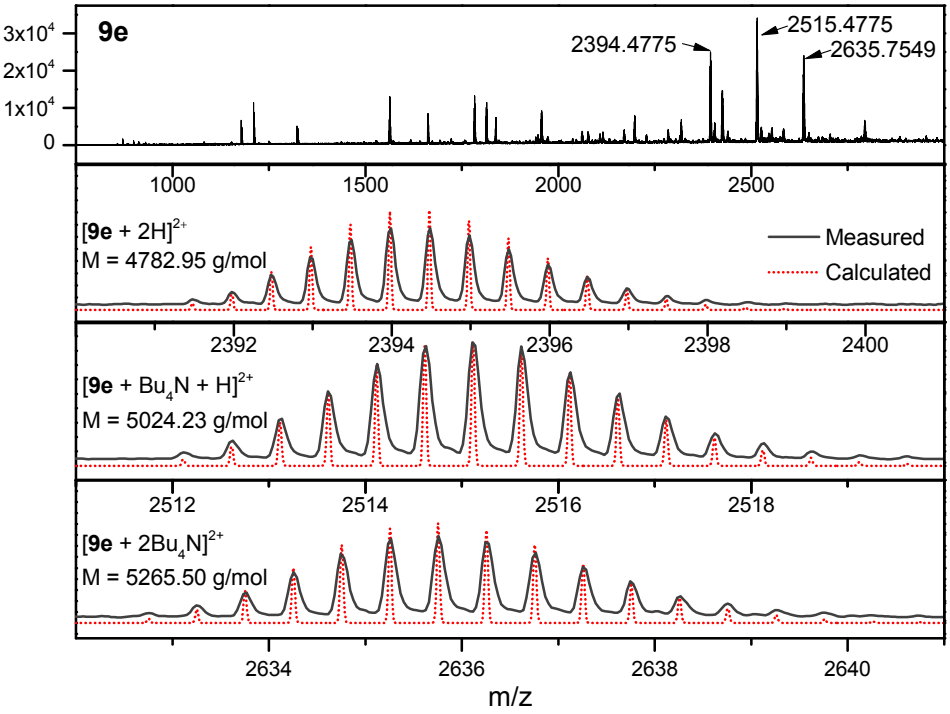

Figure S 57. ESI-MS spectrum of **9e**.

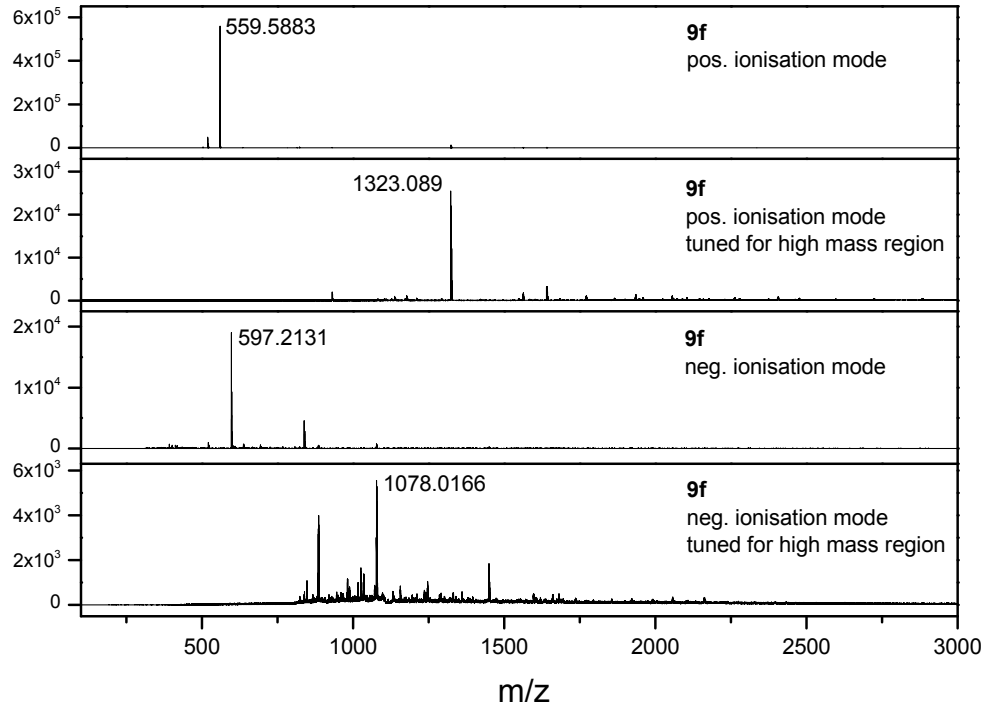

Figure S 58. ESI-MS spectrum of **9f**.

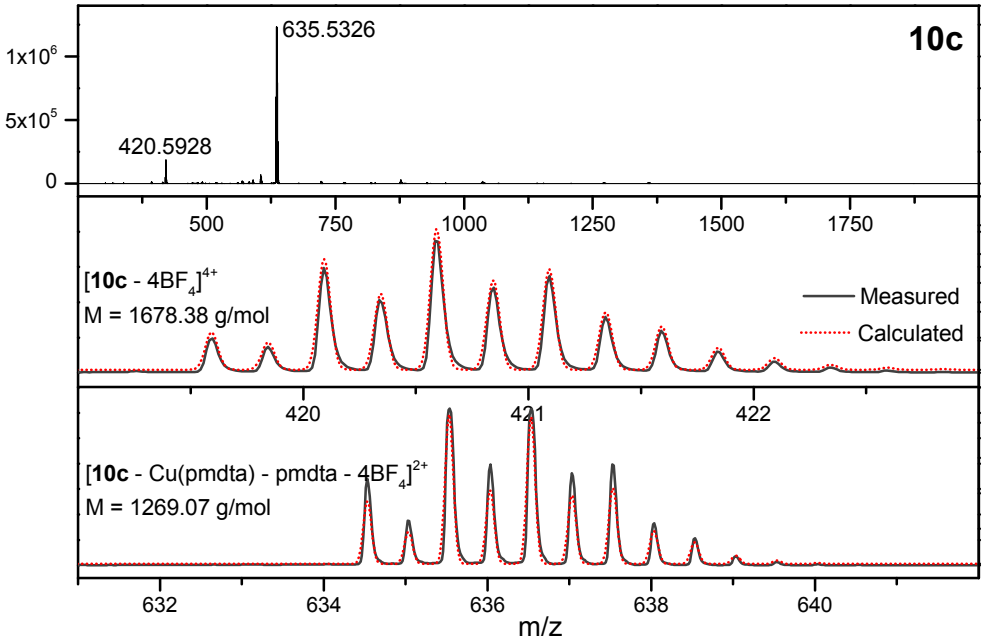

Figure S 59. ESI-MS spectrum of **10c**.

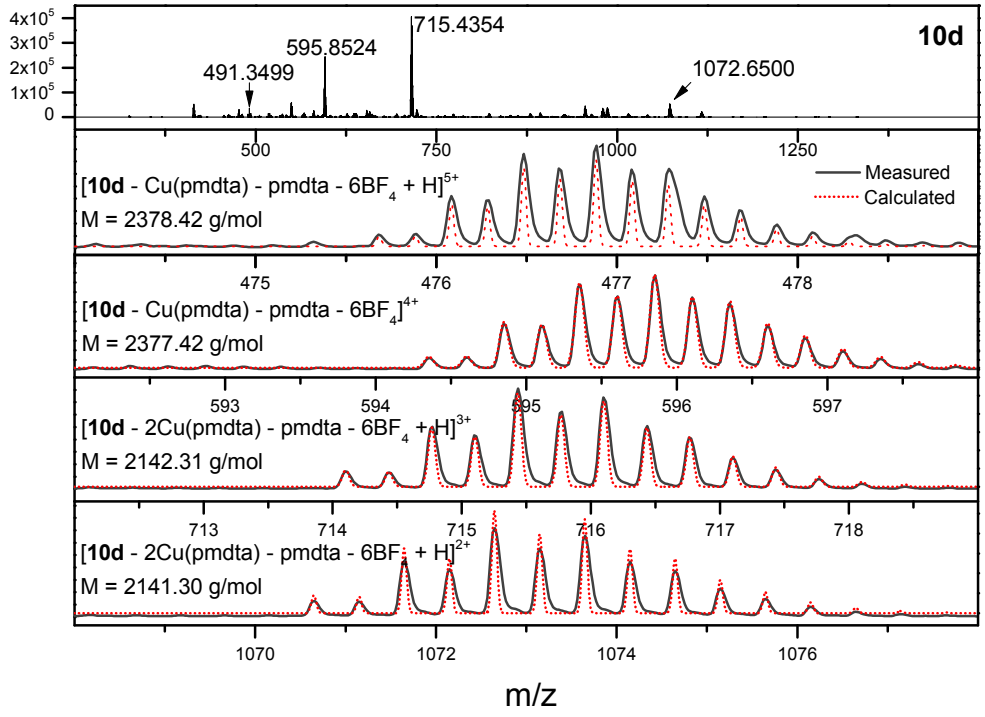

Figure S 60. ESI-MS spectrum of **10d**.

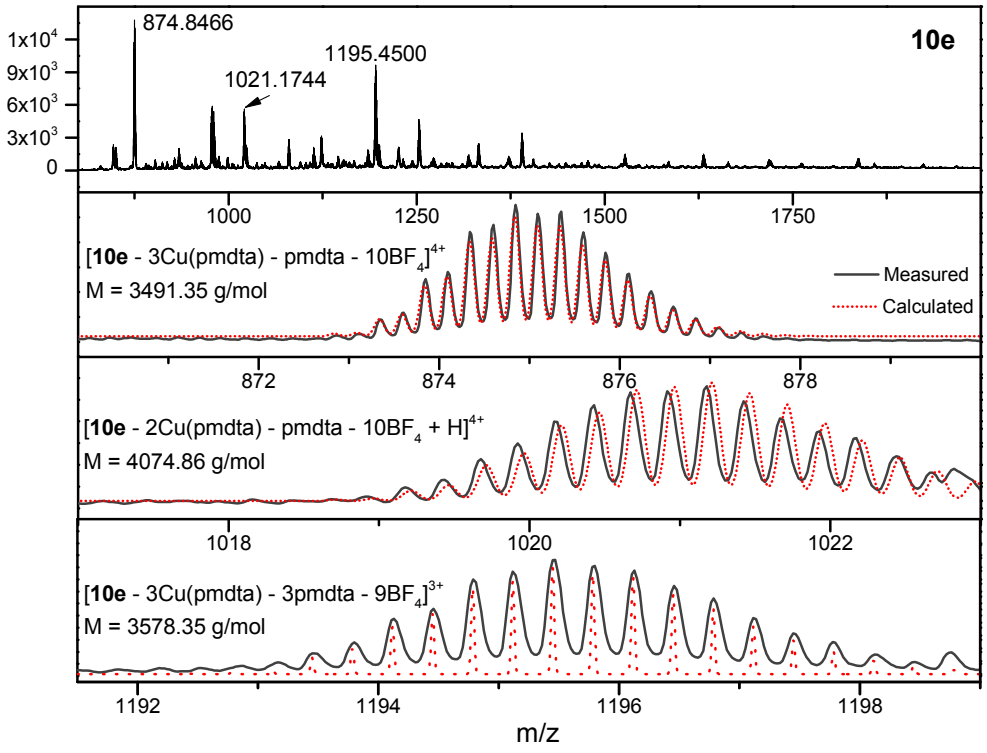

Figure S 61. ESI-MS spectrum of **10e**.

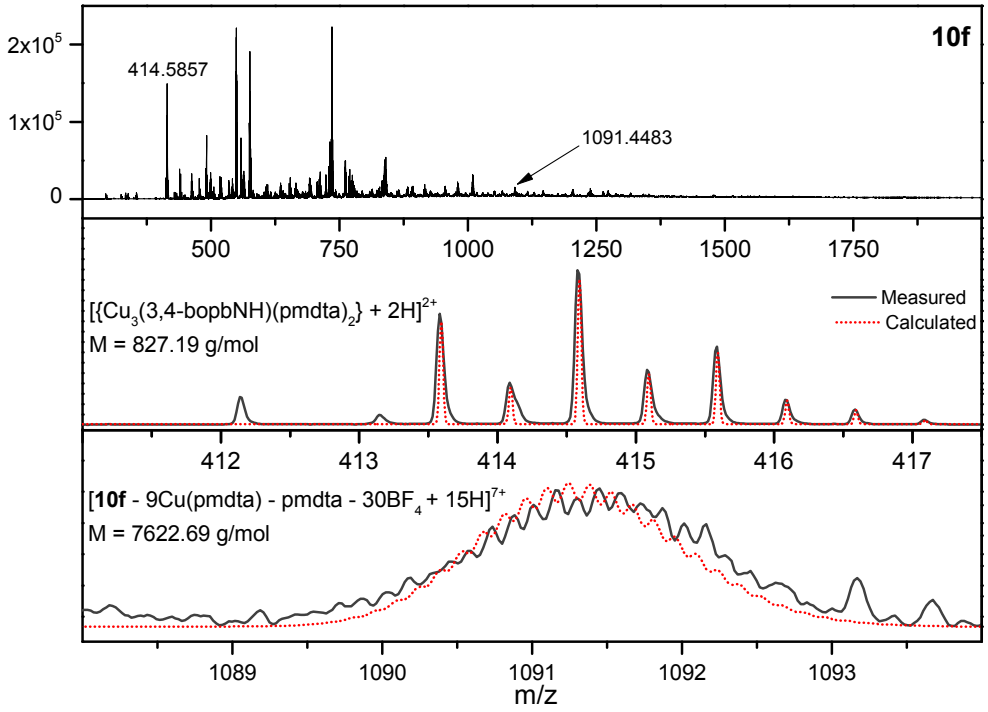

Figure S 62. ESI-MS spectrum of **10f**.

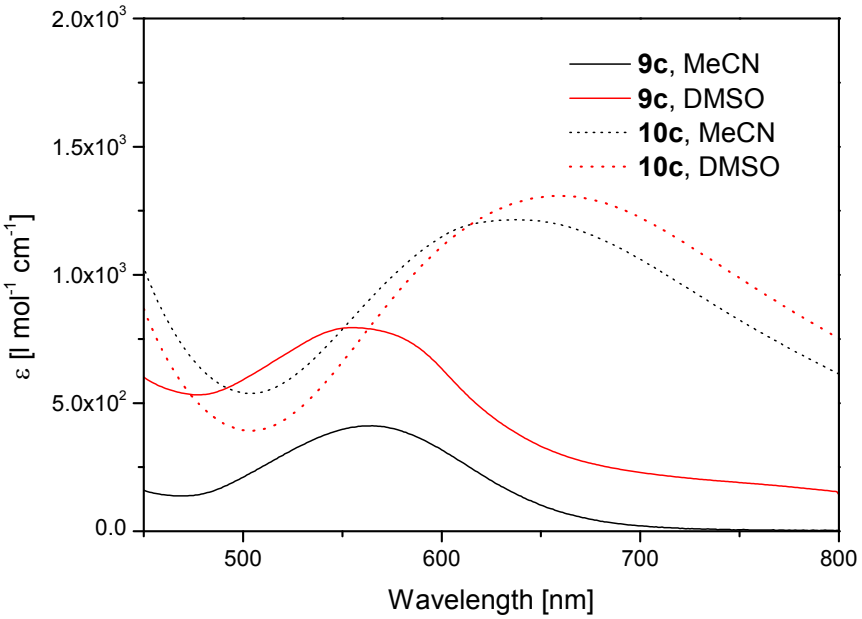

Figure S 63. Comparative UV/Vis absorption spectra of complexes **Cu-9c** (continuous lines) and **Cu-10c** (dotted lines) measured in MeCN (black) and DMSO (red).

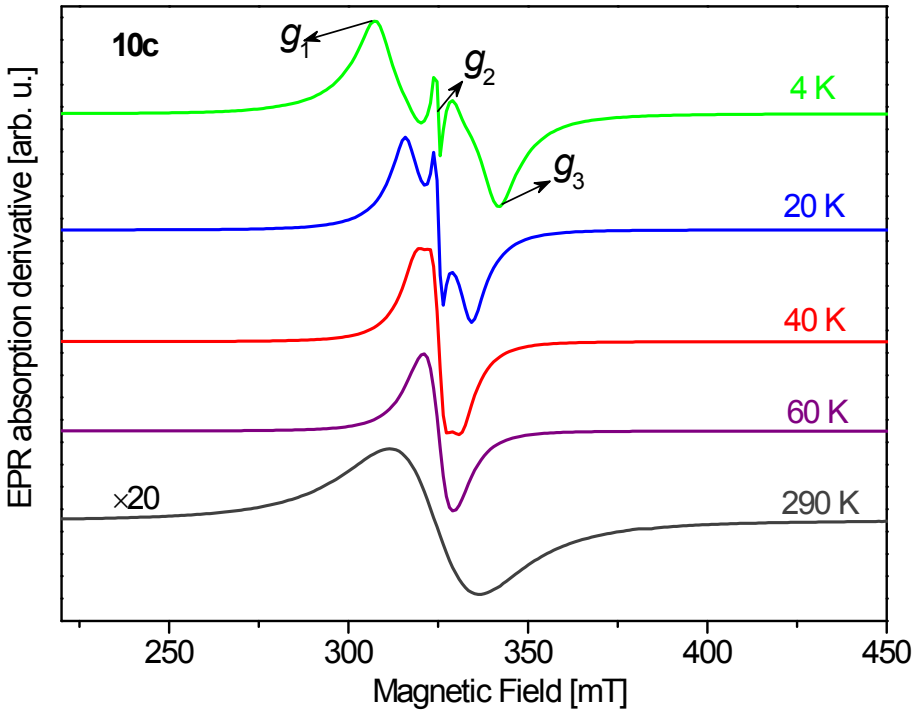

Figure S 64. Representative X-band (f = 9.56 GHz) EPR spectra of **10c** at selected temperatures. The structure of the low-T spectra is related to the three rhombic g-factors, g_1, g_2, and g_3, corresponding to the spin doublet ground state of the $\{Cu_3(3,4\text{-bopb})(pmdta)_2\}^{2+}$ entity. The broadening of the spectrum and the loss of the structure with increasing temperature is due to thermal population of the excited states.

Comment S65:

Availability of symmetric methylene diesters

As already described, the H_2O/alcohol-based reaction mixtures obtained after synthesizing mononuclear bis(oxamato) complexes were extracted with CH_2Cl_2.[1] An analogous work-up style has been applied in this case as well. The isolated complexes **Cu-3** and **Ni-3** (Scheme 1 within the manuscript), did not show any peculiarities. Single-crystal X-ray diffraction studies revealed both **Cu-3** and **Ni-3** to be binuclear complexes (Scheme 1, Figure 6 within the manuscript). Formally, both complexes represent symmetric methylene diesters. Surprisingly, the number of further crystallographically characterised symmetric methylene diesters is small.[2–4] The synthesis of those reported symmetric methylene diesters requires thereby sophisticated methods,[2,3] although it is described that simple addition of CH_2Cl_2 to [NMe(octyl)$_3$][PhCOO] affords methylene dibenzoate.[4] In this reaction, the ionic liquid [NMe(octyl)$_3$][PhCOO] is described to act as reactant, solvent and catalyst.[4] Furthermore, the conversion of tetrabutylammonium carboxylates in the presence of CH_2Cl_2, under reflux conditions and prolongated reaction times (four days), to give symmetric methylene esters is already described.[5]

In the present case, the simple extraction of the reaction mixtures, which are supposed to contain intermediates as complex **4** (Scheme 1 within the manuscript) seems to be sufficient to generate **Cu-3** and **Ni-3** as methylene diesters. This unexpected and rapid formation of methylene diester is certainly interesting to follow, but was not in the focus of the research reported here.

1 T. Rüffer, B. Bräuer, A. K. Powell, I. Hewitt and G. Salvan, *Inorg. Chim. Acta*, 2007, **360**, 3475–3483.

2 R. O. Al-Kaysi, R. J. Dillon, J. M. Kaiser, L. J. Mueller, G. Guirado and C. J. Bardeen, *Macromolecules*, 2007, **40**, 9040–9044.

3 J. Artacho, E. Ascic, T. Rantanen, J. Karlsson, C. J. Wallentin, R. Wang, O. F. Wendt, M. Harmata, V. Snieckus and K. Wärnmark, *Chem. - A Eur. J.*, 2012, **18**, 1038–1042.

4 N. V Likhanova, I. V Lijanova, L. P. M. Alvarado, M. M. García, S. Hernández-Ortega and O. O. Xometl, *Curr. Org. Chemsitry*, 2013, **17**, 79–82.

5 K. Holmberg and B. Hansen, *Tetrahedron*, 1975, **27**, 2303–2306.

Table S1. Crystal data and structure refinement parameters for **Cu-3** and **Ni-3**.

Compound	**Cu-3**	**Ni-3**
Chemical formula	$C_{180}H_{313}N_{19}O_{32}Cu_4$	$C_{180}H_{313}N_{19}O_{32}Cu_4$
Formula weight (g mol^{-1})	3509.64	3490.32
Crystal system	monoclinic	monoclinic
Space group	$P2_1/c$	$P2_1/c$
a (Å)	13.0072(2)	12.9740(3)
b (Å)	19.6446(4)	19.6759(4)
c (Å)	37.6949(7)	37.5348(8)
α (°):	90	90
β (°):	97.526(2)	97.509(2)
γ (°):	90	90
V (Å^3)	9548.9(3)	9499.5(4)
Z	2	2
Measurement temperature (K)	100	100
Radiation source	Cu Kα	Cu Kα
Wavelengths (Å)	1.54184	1.54184
D_{calc} (g cm^{-3})	1.221	1.220
μ (mm^{-1})	1.074	1.020
F(000)	3796	3788
Reflections collected	48943	36627
Reflections unique/R_{int}[a)]	15913/0.0225	15813/0.0236
Index ranges	$-15 \le h \le 15$,	$-15 \le h \le 13$,
	$-23 \le k \le 22$,	$-23 \le k \le 23$,
	$-44 \le l \le 39$	$-44 \le l \le 43$
θ range for data collection (°)	4.101 – 64.991	3.436 – 64.995
Data / restraints / parameters	15913 / 8 / 1093	15813 / 0 / 1103
Goodness–of–fit on F^2 [b)]	1.055	1.032
Final R indices [$I > 2\sigma(I)$][c)]	$R_1 = 0.0622$	$R_1 = 0.0673$
	$wR_2 = 0.1711$	$wR_2 = 0.1917$
R indices (all data)[c)]	$R_1 = 0.0776$	$R_1 = 0.0844$
	$wR_2 = 0.1813$	$wR_2 = 0.2028$
Largest diff. peak, hole (e Å^{-3})	0.825/–0.486	0.833/–0.408

[a)] $R_{int} = \Sigma \left| F_o^2 - F_o^2(\text{mean}) \right| / \Sigma F_o^2$, where F_o^2(mean) is the average intensity of symmetry equivalent diffractions. [b)] $S = [\sum w(F_o^2 - F_c^2)^2]/(n-p)^{1/2}$, where n = number of reflections, p = number of parameters. [c)] $R = [\sum(||F_o| - |F_c|)/\sum|F_o|]$; $wR = [\sum(w(F_o^2 - F_c^2)^2)/\sum(wF_o^4)]^{1/2}$.